

oml

OAK
RIDGE
NATIONAL
LABORATORY

UNION
CARBIDE

OPERATED BY
UNION CARBIDE CORPORATION
FOR THE UNITED STATES
DEPARTMENT OF ENERGY



3 4456 0133564 9

ORNL-5760

Final Report on Cermet High-Level Waste Forms

E. H. Kobisk
T. C. Quinby
W. S. Aaron

OAK RIDGE NATIONAL LABORATORY

CENTRAL RESEARCH LIBRARY

CIRCULATION SECTION

FORM 708-11

LIBRARY LOAN COPY

DO NOT TRANSFER TO ANOTHER PERSON

If you wish someone else to see this
report, send its name with report card
the library will arrange a loan.



3 4456 0133564 9

ORNL-5760
Dist. Category
UC-70

Contract No. W-7405-eng-26

Solid State Division

NUCLEAR FUEL AND WASTE PROGRAMS

FINAL REPORT ON CERMET HIGH-LEVEL WASTE FORMS

E. H. Kobisk, T. C. Quinby, W. S. Aaron

Date Published: August 1981

OAK RIDGE NATIONAL LABORATORY
Oak Ridge, Tennessee 37830
operated by
UNION CARBIDE CORPORATION
for the
DEPARTMENT OF ENERGY

CONTENTS

	<u>Page</u>
LIST OF TABLES.	iv
LIST OF FIGURES	v
ABSTRACT.	1
INTRODUCTION.	1
BACKGROUND TECHNOLOGY	3
CERMET FORMULATIONS	7
PROCESSING DEVELOPMENTS	12
Reactive Spray Calcination.	15
Cermets Densification Methods.	24
Summary	30
VOLATILITY LOSS STUDIES	32
CERMET LEACHABILITY	35
PROCESSING CHARACTERISTICS AND VARIOUS CERMET PROPERTIES. .	48
Waste Loading	48
Waste Volume Reduction.	49
Metal-to-Ceramic Ratios	49
Density	50
Thermal Conductivity.	50
Decay Heat Loading.	50
Oxidation Behavior.	50
Thermal Shock Resistance.	51
APPLICATION OF CERMETS TO SPACE DISPOSAL OF NUCLEAR WASTES.	51
ACKNOWLEDGMENTS	54
REFERENCES.	55

LIST OF TABLES

<u>Table</u>		<u>Page</u>
1	Chemical Analyses of NFS Acid Thorex Waste and Resulting Cermet Formulation	9
2	Reactive Spray Calciner Off-Gas Analysis	18
3	Typical Calcine Particle Size Distribution	23
4	Volatility Losses of Cs and Ru During Processing of Fresh SRP Acid Waste	35
5	Results of PNL Leach Tests A, B, C	43
6	Preliminary Galvanic Series Results in WIPP "B" Solution	47

LIST OF FIGURES

<u>Figure</u>		<u>Page</u>
1	Flowsheet of the urea-based process for preparation of ceramic dosimeter wires	4
2	SEM micrographs of ceramic wires produced by the extrusion and sintering of submicron calcine powder a) Pure ThO ₂ showing extrusion artifact b) 0.13 wt. % Sc as scandium oxide in MgO c) 5.5 wt. % Th as ThO ₂ in MgO.	6
3	Original laboratory-scale operations used to produce cermet waste form samples	13
4	Improved flowsheet for cermet preparation developed to permit simpler and scalable operations.	15
5	Schematic diagram of the reactive spray calciner including one of the optional methods for calcine collection. . .	20
6	Schematic representation of the nozzle used for the spray calcination of molten urea solutions.	21
7	The narrow, well atomized spray pattern provided by the nozzle (Fig. 6) permits effective calcination of molten urea solutions.	21
8	a) SEM micrograph of typical calcine particles b) Reactive spray calcination using an inert injection gas results in partial, if not complete, reduction of metal species as indicated by the ductility of this mechanically deformed particle (bar length represents 50 μm)	25
9	Schematic illustration of mechanism for liquid phase sintering of cermets.	29
10	Typical temperature-time profiles for conventional and liquid phase sintering show some of the advantages of the latter.	29
11	Comparison of microstructures of actual waste cermet samples prepared by different sintering techniques a) NFS Acid Thorex Waste - conventional sintering b) SRP Acid Waste - liquid phase sintering	31

<u>Figure</u>		<u>Page</u>
12	Scrubber columns attached to calcination furnace which were installed in a hot cell for actual waste volatility studies	33
13	Leaching apparatus for early radiotracer leach tests at ORNL.	39
14	Percolator used for leachant circulation in early radiotracer leach tests at ORNL. Resulting abrasion of sample surface proved unsatisfactory	40
15	Macrograph of cermet sample surface following Soxhlet leach testing shows essentially no change in appearance as a result of the test	43
16	Macrograph of cermet sample surface following 146-day leach test. Apparent galvanic coupling with stainless steel mesh basket resulted in surface deposits on the cermet sample	45
17	SEM micrograph of the cross section of the 146-day leach test sample shows minimal attack of cermet, even in areas where deposits of "rust" occurred as a result of apparent galvanic coupling	46
18	SEM micrograph of the cross section of the hydrothermal brine leach test sample showing the thin, adherent reaction layer which developed on the cermet surface. . .	46

FINAL REPORT ON CERMET HIGH-LEVEL WASTE FORMS

E. H. Kobisk, T. C. Quinby, W. S. Aaron

ABSTRACT

Cermets are being developed as an alternate method for the fixation of defense and commercial high level radioactive waste in a terminal disposal form. Following initial feasibility assessments of this waste form, consisting of ceramic particles dispersed in an iron-nickel base alloy, significantly improved processing methods were developed. The characterization of cermets has continued through property determinations on samples prepared by various methods from a variety of simulated and actual high-level wastes. This report describes the status of development of the cermet waste form as it has evolved since 1977.

INTRODUCTION

In August of 1977, a program was undertaken by the Isotope Research Materials Laboratory (IRML) of the Oak Ridge National Laboratory to develop a cermet process for high-level waste solidification and to evaluate the resulting cermet waste form. The cermet waste form is designed to provide fixation of high-level wastes as multimicron-size oxide particles or tailored, crystalline compound particles uniformly dispersed in a corrosion-resistant, thermally conductive, metal alloy matrix. This process has been successfully applied to both commercial and DOE defense wastes. The process used to form cermets from high-level

wastes possesses many unique and advantageous features, as does the cermet itself. During processing, significant waste volume reductions and high waste loadings are achievable, while volatility losses of radioisotopes, such as Cs, Ru, and Sr are kept very low. Resulting cermets have been shown to possess high thermal conductivity, leach resistance, excellent durability under high pressure-temperature conditions and good mechanical strength.

Developmental work was performed using simulated wastes, radiotracer-containing simulated wastes and actual Nuclear Fuel Services (NFS) Acid Thorex, Savannah River Plant (SRP) dried sludge and fresh, unneutralized SRP acid wastes. Following the controlled and monitored processing of these various wastes into cermets, substantial sample characterization work was performed. Thermal conductivity determinations, calorimetry (for actual wastes only), optical and scanning electron metallography, x-ray energy spectroscopy and, in some cases, x-ray diffraction were among the methods used to characterize the cermets. Leach tests and high temperature-pressure durability tests have been performed at Battelle-Pacific Northwest Laboratories in addition to the work done at ORNL. Engineering, economic, and safety analyses of both the cermet process and the product were conducted on a preliminary basis; however, additional development effort would be required before a definitive analysis could be completed.

In this report, the cermet process and resulting waste form(s) will be described and the progress of the program, previously reported [1], will be updated.

BACKGROUND TECHNOLOGY

Since 1971, IRML has been involved in the development and preparation of neutron dosimeter materials using a process which was later adapted to the preparation of cermets [2,3]. The process used to prepare these dosimeter materials will be described briefly to clarify process steps similar to those used for the preparation of waste-containing cermets. The same basic process has also been used for a wide variety of other special materials preparations.

Neutron dosimeters referred to in this discussion consist of a wide variety of pure and diluted oxides in the form of ceramic wires which are loaded into small, high-purity vanadium capsules and sealed by welding. Dosimeters are then placed in a reactor core and irradiated for varying times. Post-irradiation analysis in combination with very accurate pre-irradiation characterization permits the calculation of the neutron flux and energy distribution throughout the reactor core. Fissile and stable materials in either the pure form or diluted in an inert carrier material, such as MgO or Al₂O₃, have been prepared as ceramic wires. In the case of target oxide dilutions, a prime requirement is the uniformity of distribution of the target nuclides in the diluent. A typical uniformity tolerance for such dilutions is a less than 1% variance from the mean concentration of the target oxide composition, ranging as low as 0.1 wt. %, over a batch length of 610 m (2,000 ft.) of 0.05 cm (0.020 in.) diameter wire. A flowsheet for the preparation of ceramic oxide wires is shown in Fig. 1. The desired components in their appropriate relative quantities are first dissolved in nitric acid to obtain a mixed nitrate solution which is then heated to concentrate the

ORNL-DWG 77-15817

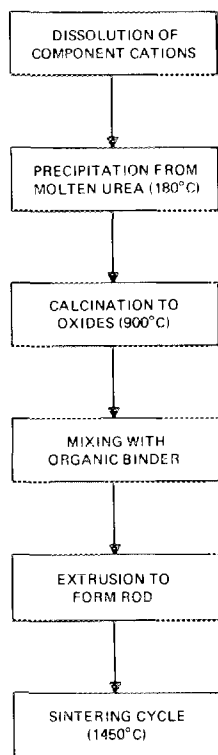


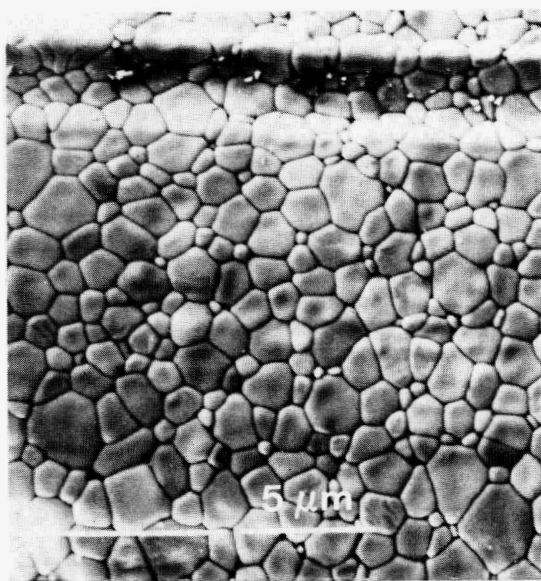
Fig. 1. Flowsheet of the urea-based process for preparation of ceramic dosimeter wires.

solution. Urea is then added to the solution and heated; in this process step residual water, including water of hydration, is removed through reaction with the urea or direct volatilization. Denitration of the solution occurs simultaneously and, as heating continues, it is postulated that some of the urea polymerizes through the linking of $-NH_2$ groups and simultaneous evolution of NH_3 . Homogeneously mixed component cations are evidently incorporated in the polymerized material. The resulting polymer or urea coprecipitate is subsequently calcined to remove volatile species and to convert the desired components to their oxides, which, because of the urea coprecipitation step, are intimately and homogeneously mixed. Because this process yields submicron size

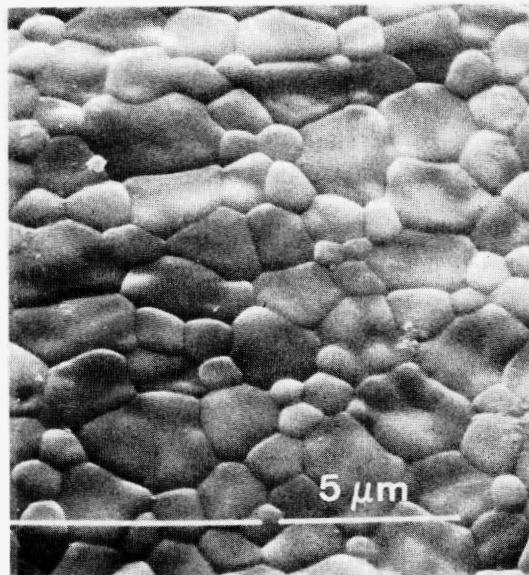
particles in a controllable manner, the chemical precipitation process enhances the sinterability of many difficult-to-sinter oxides without introducing chemical impurities as might occur when mechanical particle size reduction methods are employed. Introduction of impurities would be generally detrimental to subsequent use in neutron dosimetry.

Following calcination, the oxide powder is mixed with a binder, typically a wax, and extruded to form a wire which, after sintering and shrinkage of approximately 25%, will be of the desired final size. The "green" extruded wire is sintered at temperatures of up to 1450°C. The sintering cycle usually includes a slow heat-up procedure during which the binder is volatilized and typically includes an 8-12 hour holding period at the maximum temperature so as to permit sintering to densities of up to 96% of theoretical density for many materials. Scanning electron micrographs shown in Fig. 2 illustrate typical structures of several sintered ceramic wires.

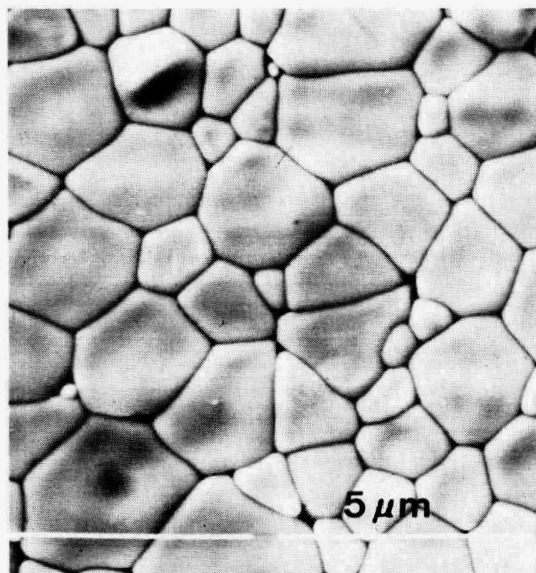
Other materials applications employing all or parts of this processing technology include preparation of catalyst supports and coprocessing of the catalyst with the support, the fabrication of $^{244}\text{Cm}_2\text{O}_3$ rectangular bars for materials compatibility studies, and the preparation of MgO crucibles used in uranium fluorescence analyses (as a substitute for Pt crucibles which require one crucible per analysis and are not reusable). Investigations to determine the applicability of this process to the preparation of mixed oxides, including reactor fuels, and a wide range of cermets are also being conducted. A solid solution alloy of 50 wt. % Cu - 50 wt. % Ni was prepared by coprecipitation from urea, calcination of the precipitate to the oxides and hydrogen reduction.



(a)



(b)



(c)

Fig. 2. SEM micrographs of ceramic wires produced by the extrusion and sintering of submicron calcine powder.

- a) Pure ThO_2 showing extrusion artifact
- b) 0.13 wt. % Sc as scandium oxide in MgO
- c) 5.5 wt. % Th as ThO_2 in MgO

of the oxides to metals at 800°C. X-ray diffraction confirmed the formation of a completely uniform, solid solution alloy of the Cu and Ni which is evidence of the excellent homogeneity of mixing obtained from the molten urea coprecipitation process.

Application of this technology to radioactive wastes was initiated after the successful processing of a variety of chemical elements and mixtures of elements. It was also realized that selective reduction of metal oxides in an oxide mixture obtained through urea precipitation and calcination would yield an intimate mixture of the ceramic and metal phases. Upon densification of these oxide-metal mixtures, cermets could be obtained with a wide variety of controlled compositions and properties. Cermet properties are determined primarily by the chemical components added; however, processing methods, particularly changes in parameters associated with the reduction and densification procedures can have significant effects as well. Syntheses of tailored oxides (mineral compound forms) and alloys are possible using this process, and it is the features which are being exploited for the fixation of high-level radioactive wastes in a cermet waste form.

CERMET FORMULATIONS

Cermets are designed to offer two barriers to the release of radioactive wastes, whether it be by leaching, impact, or high temperature degradation. This is achieved by the formation of stable, highly insoluble ceramic phases and an inert alloy matrix which microencapsulates the ceramic particles. While it would be repetitive to review all the waste compositions that have been investigated, the discussion of one such example will illustrate the method by which the formulation

of the cermet is derived. It should be noted that the cermet formulation to be discussed has not been chosen as being optimum. It simply appears satisfactory at the level of development achieved to date. Wastes, in general, are grossly inhomogeneous and only in a few instances have they been thoroughly characterized. For these reasons, careful monitoring of waste compositions as they enter the process must be performed (as with other candidate processes) to accommodate compositional changes within reasonable limits.

In 1978 a sample of NFS acid Thorex waste was drawn from the tankage at the West Valley, New York, site and transported to ORNL for analysis and subsequent conversion to cermet. The chemical composition of this waste is shown in Table 1 in terms of both the elemental concentrations in the waste and the expected form and weight of these elements as they would exist in a cermet formed from a volume of 31 ml of this acid waste. The additives required to formulate the desired cermet are also shown.

In general, it is desirable to form a cermet having approximately 50% by volume metal to maintain the thermal conductivity and mechanical strength of the body. Cermets have been formed using pure Ni, Fe-Ni alloy bases, and Fe-Ni-Cu-Co (Mo) alloys. The choice of the alloy composition is ultimately dependent upon required compatibility with the proposed storage environment specific to a particular repository or disposal method and the availability of reducible metals either already in the waste or added at the head-end of the process. The metal alloy will contain reducible fission products from the waste which will vary in quantity and type depending on the waste being considered. As shown in the example, this cermet has an alloy phase composition of 70-Fe, 20-Ni, 5-Cu, 5-Co, and small amounts of miscellaneous reducible fission products.

Table 1. Chemical Analysis of NFS Acid Thorex Waste and Resulting Cermet Formulation

<u>Waste</u>		<u>g/l</u>	<u>Desired Form</u>	<u>Desired Form Weight (g)</u>
Metal Formers:	Fe	49	Metal	1.519
	Ni	7.18	Metal	0.223
	Ru	0.57	Metal	0.018
	Mo	0.55	Metal	0.017
	Zn	0.18	Metal	0.005
	Cu	0.06	Metal	0.002
	Co	0.03	Metal	0.001
Ceramic Formers:	Cr	1.07	Cr ₂ O ₃	0.485
	K	1.66	KAlSi ₂ O ₆	0.288
	Na	6.4	NaAlSi ₂ O ₆	1.745
	Th	228	ThO ₂	8.052
	Al	10	(Na, K, Rb, Cs) AlSi ₂ O ₆ + Al ₂ O ₃	Undetermined
	Rare Earths	1.98	RE ₂ O ₃	0.072
	Cs	0.70	CsAlSi ₂ O ₆	0.121
	Ba	0.50	BaTiO ₃	0.026
	Mn	0.85	MnO	0.034
	Zr	0.12	ZrO ₂	0.005
	Sr	0.18	SrTiO ₃	0.012
Rb	0.08	RbAlSi ₂ O ₆	0.018	

Table 1. (Cont'd)

<u>Additives:</u>	<u>Element</u>	<u>Elemental Weight</u>	<u>Form</u>
Metal Formers	Fe	18.08	Metal
	Ni	5.38	Metal
	Cu	1.40	Metal
	Co	1.40	Metal
Ceramic Formers	Al	0.10	(Na, K, Rb, Cs) $AlSi_2O_6 + Al_2O_3$
	Si	0.86	(Na, K, Rb, Cs) $AlSi_2O_6 + SiO_2$
	Ti	0.44	(Se, Ba) $TiO_3 + TiO_2$

The alloy composition can be easily modified since it can be made from any mixture of reducible metals added to the waste to obtain appropriate metal phase properties.

The amount of additives required to fix specific fission products and inert nuclides in the waste as insoluble ceramics must be determined. Aluminum and silicon are added to fix the Na, K, Rb, and Cs, in the waste as (Na, K, Rb, Cs) $AlSi_2O_6$ (pollucite). Additions of aluminum and silicon are made, when required, to supplement the amount of these materials already in the waste, in order to provide a 50% stoichiometric excess of aluminum and silicon. This is done to ensure compound formation and to provide for variability in the composition of the waste. Excess material additions also ensure that if any segregation of Na, K, Rb, and Cs occurs during processing prior to the formation of the pollucite compound,

there will be sufficient aluminum and silicon present to permit the formation of the mineral in localized areas. It is expected that lower excess additions probably would provide satisfactory results. Likewise, titanium additions are made in excess of the amount required to form titanates from the Ba and Sr present in the waste, with the remainder forming TiO_2 . It should be necessary to add only a 10-50% excess of titanium to achieve total fixation.

The above formulation resulted in a cermet having a total waste loading of approximately 28 wt. %. The metal phase was approximately 69 wt. % of the final cermet, while 31 wt. % consisted of mixed ceramic phases.

This example illustrates the general considerations used to formulate waste cermet compositions. Since portions of the waste are used to form the metal matrix of the cermet (as compared with the totally independent metal matrix used in the multibarrier waste concept), the formulation of the cermet is dependent on the composition of the specific wastes. Minor compositional changes are easily accommodated by the cermet waste form. In the case of PW-4b waste, on which laboratory-scale investigations have been initiated only recently, the metal phase contains a larger amount of fission product metals and a significantly different mixture of ceramic phases. Since the cermet metal alloy matrix composition varies with each type of waste, these various matrices must be evaluated to ascertain their integrity, especially with respect to leach resistance. While not considered in this example, it has been shown that with additions of phosphate ion, monazites can be formed as a host ceramic phase. Monazites are currently being prepared using the urea process for investigations conducted by Boatner and co-workers at ORNL [4]. Likewise, the urea process

has also been applied to Synroc preparation at LLL [5]. This process therefore provides great flexibility in the selection of ceramic phases for waste fixation limited only by the thermodynamic stability of the various phases coexisting during late stages of processing and in the final waste form.

PROCESSING DEVELOPMENTS

Processing steps required for the preparation of cermets are similar to those previously described for ceramic wire and related materials. The basic process was presented earlier [1] but has since undergone appreciable development. Significant improvement and simplification of the batch-type cermet process has been achieved and, more recently, efforts have been concentrated on development of a continuous process suitable for engineering scale-up.

A flowsheet of the batch process for cermet preparation is shown in Fig. 3 along with materials additions as are required in the process and the products generated during the process. The first step of this process involves the dissolution of all components in nitric acid, including the waste material and specific additives as required for the formation of desired crystalline compounds, such as aluminosilicates and titanates. Formulation of the desired composition for the metal alloy phase in the final cermet is also performed in this dissolution step. The solution is then concentrated by heating and urea is added. With continued heating, the molten urea solution undergoes reactions which produce a solid precipitate and the gaseous products shown on the flowsheet. This solid precipitate is then calcined to decompose metastable compounds and convert all species to oxides. Various methods have been used to convert

the reducible metal oxides to metal and densify the material into the final cermet waste form.

During the course of developmental studies, a number of improvements were made to the batch flowsheet and many advantageous features, unique to urea processing, were recognized. It was found that most wastes, zeolites and additives may be dissolved directly in molten urea and, therefore, nitric acid need not be added. When the nitric acid step is eliminated, the metal additives must be in a soluble form, e.g., nitrates or other

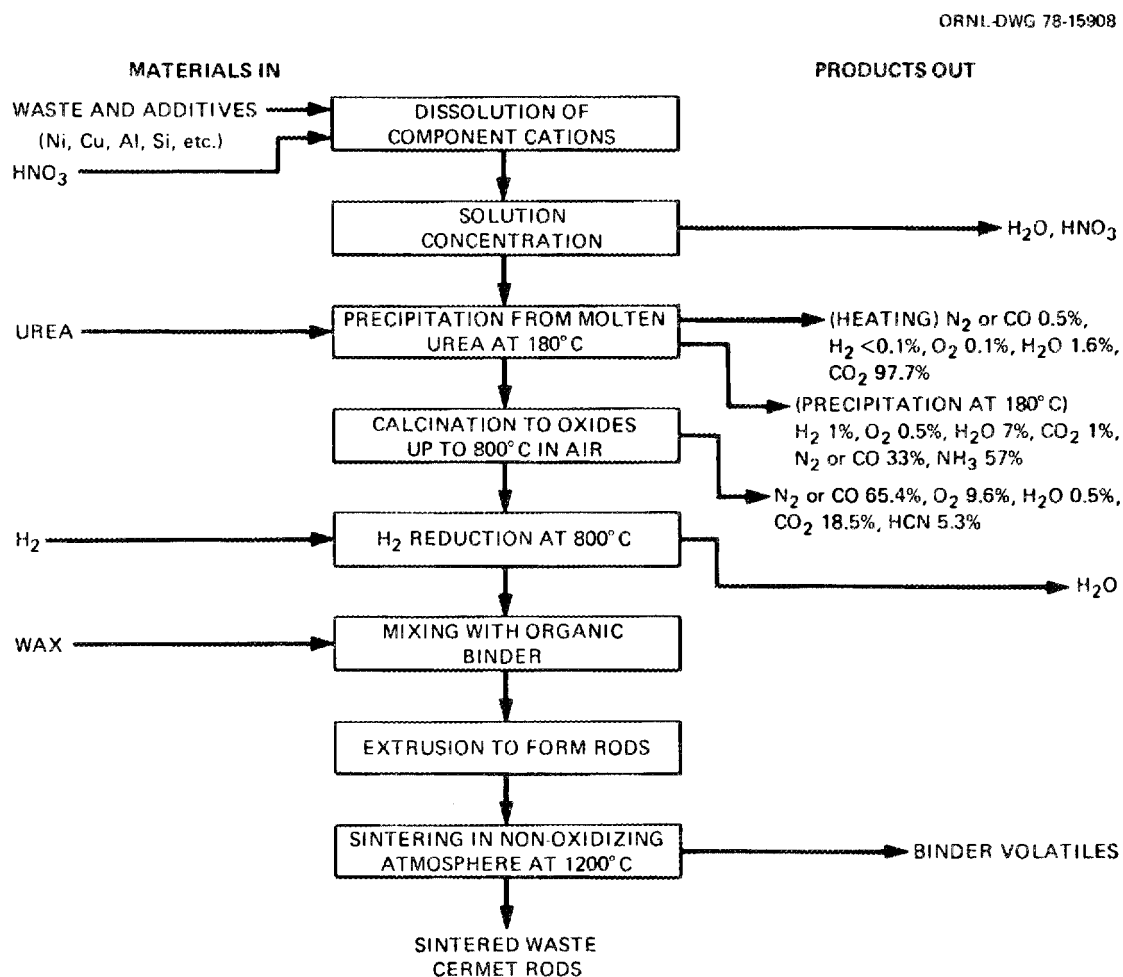


Fig. 3. Original laboratory-scale operations used to produce cermet waste form samples.

salts, since most of metals are insoluble or have a low dissolution rate in molten urea. Investigations have been conducted on the effects of varying the relative amount of urea used for the precipitation process. The exothermic nature of the precipitation reactions requires a minimum 5:1 molar ratio of urea-to-nitrate ion in order to control the reaction in the batch process. The total nitrate ion concentration of the solution arises from both the waste and the additives. Lower urea ratios result in the boil over of material from its container (beaker). A dependence of product particle size on the urea-to-nitrate ratio was found to exist as that ratio was varied from 5:1 to 45:1. As the ratio is increased, the size of the resulting precipitate and subsequent calcine particles is reduced. It is postulated that the exothermic reaction provides the heat necessary to initiate reaction of adjacent volumes in the molten urea. As the relative urea content is increased, this exothermic reaction is "diluted" with more and smaller volumes of solution being reacted to form finer precipitating particles. In this case, the exothermic heat is expended, in part, to heat up adjacent volumes of urea and is therefore not available to trigger the reaction between the urea and nitrate ions in large volumes of the solution. The control offered by high urea-to-nitrate ion ratios, while necessary in batch processing, is not required or even desirable in the spray calcination of molten urea solutions (as discussed below).

All products of the precipitation and calcination processes are either gases or solids with no liquid effluents except those generated by off-gas handling equipment (scrubbers). All gaseous products generated during batch processing are innocuous except for small amounts of HCN produced during calcination, as shown in the right column of the

flowsheet (Fig. 3). Reaction gases may also contain very small amounts of volatilized radioisotopes, such as Cs and Ru, the volume of which is minimized by the reducing environment produced and maintained by the urea during early stages of the process. Low volatility losses are also observed during the various densification methods that will be discussed below in greater detail. Experimental results concerning volatility losses are presented in a separate section.

Reactive Spray Calcination

Transformation of the laboratory-scale, batch cermet process into one which incorporates reliable unit operations amenable to remote operation and engineering scale-up has been studied. A continuous-type process, as illustrated in Fig. 4, is suggested for the full-scale processing of radioactive waste. One of the key unit operations for successful continuous processing appears to be associated with the precipitation and calcination steps. Experimentally it was found that these two operations could be combined through the use of a heated-wall rotary calciner into

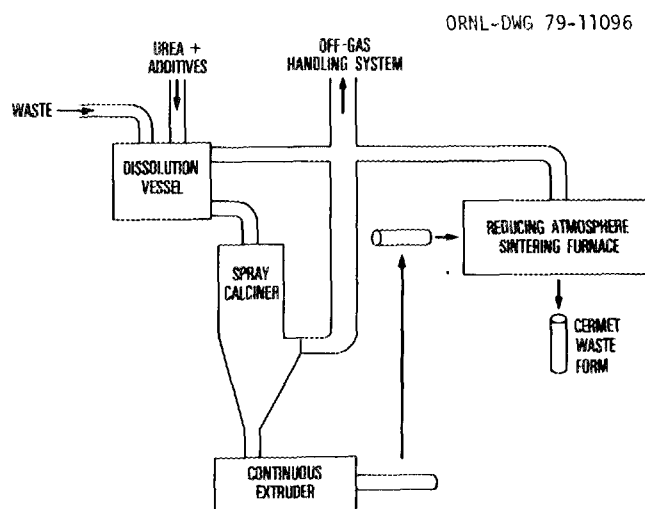


Fig. 4. Improved flowsheet for cermet preparation developed to permit simpler and scalable operations.

which the molten urea solution was fed. Both precipitation and calcination processes take place in this single operation, resulting in an oxide powder calcine. The calcine was somewhat agglomerated, however; to alleviate this problem, a "reactive" spray calciner was designed and fabricated in an effort to form a more finely divided product which would facilitate subsequent densification. The term, "reactive", is applicable since spray calcination of urea-containing solutions, and the associated chemical reactions which occur, is significantly different than conventional spray calcination, although the equipment required is very similar.

A reactive spray calciner having a 10-cm i.d. was operated successfully using simulated waste-urea feed solutions. As expected, the spray calciner produced a powder consisting of generally spherical particles up to approximately 10 μm in diameter when a urea-to-nitrate mole ratio of 1:1 was used. Urea-to-nitrate ion ratios were lowered from 5:1 to 1:1 to reduce material additions and the quantity of off-gas generated, since the reaction rate control provided by the higher ratios (as required for batch processing) was not needed or desired for spray calcination. As in batch processing, particle size resulting from spray calcination was dependent on the amount of urea added per unit of waste. The mechanism for this particle size dependence is different however from that described previously for batch processing. As the amount of urea increases, the resulting particle size decreases, since, for a given size spray droplet, the amount of the solid-forming material in the droplet decreases.

In addition to simplifying the cermet preparative flowsheet by combining two process steps into one, an even more significant advantage of spray calcining is the reduction in the amount of urea required as compared to batch processing. Whereas in batch processing, excess urea was required to slow the exothermic urea-nitrate reaction to a controllable rate, in the spray calciner it is desirable to have the reaction proceed very rapidly so that "precipitation and calcination" occurs during the short residence time of the material in the calciner. Heat provided by the exothermic reaction in the spray calciner also minimizes the heat which must be supplied to the calciner walls. Using a urea-to-nitrate mole ratio of 1:1, centerline temperatures in the calciner can be maintained at or slightly below the wall temperature. It has also been found that calcination occurs so rapidly that the material is converted to dry powder before it comes in contact with the calciner walls. Therefore, no material buildup occurs on the walls of the calciner such as occurs in spray calciners using waste solutions not containing urea; such deposits must then be loosened by an air-operated vibrator mounted on the calciner wall [6].

Another significant difference in using reactive spray calcination was noted when resultant off-gases were analyzed. While batch processing yielded off-gases of varying compositions as the precipitation and calcination stages proceeded, the off-gas from the spray calciner reached and maintained a steady state composition, since precipitation and calcination steps take place essentially instantaneously and continuously. The actual spray calciner off-gas composition resulting from an analysis of gases generated during a test using simulated NFS acid Thorex waste with a 1:1 urea-to-nitrate mole ratio is shown in Table 2. It can be

seen that the species generated during spray calcination are significantly different and even more innocuous than those resulting from equivalent batch-type operations. Notably, no HCN was detected and ammonia was essentially nonexistent. Only insignificant amounts of H₂ and NO_x were found to be present.

A 20-cm i.d. reactive spray calciner was installed to permit more flexibility in operation and a more thorough evaluation of operating parameters. During testing of the 10-cm i.d. calciner, it was found that the small diameter resulted in very little flexibility for parametric studies such as the influences of feed rate and spray pattern. No radiotracer studies were performed to determine possible losses of radioactive species in this process.

Table 2. Reactive Spray Calciner Off-Gas Analysis

<u>Species</u>	<u>Concentration</u>
N ₂ and/or CO	75.09% (in separate analysis CO <0.43%)
H ₂ O + NH ₃	11.95% (no evidence of NH ₃ during processing)
CO ₂ and/or N ₂ O	2.56%
O ₂	9.39%
NO	0.77%
H ₂	0.17%
NO ₂	<0.09%

It appears that the reactive spray calciner can be operated in either of two modes depending on the type of calcine needed for subsequent densification. In some cases, it is desirable to start with a calcine in which the reducible metal species are present as the respective elements, thus yielding a fine, homogeneous powder mixture of metal and oxide suitable for subsequent densification. There is evidence to indicate this may be accomplished by operating the calciner as a closed system with an inert injection gas. Under these conditions, it appears possible to maintain a sufficiently reducing atmosphere to produce the mixed metal-oxide powder. In preliminary tests, partial, if not complete, reduction was achieved through the use of argon as the injection gas. For other methods of densification, an oxide powder is the preferred form of starting material. This mode of operation has been used with the calciner being operated as an "open" system, with air being used as the injection gas.

The reactive spray calciner is shown in Fig. 5. The liquid waste feed is composed of the waste and additives dissolved in the appropriate amount of urea. This feed solution is formed in a heated dissolution vessel where dissolution and homogenization of the waste and additives in urea take place. The feed solution must generally be heated since the melting point of urea is 405 K. The melting point is lowered with increasing water content and it has been the practice to maintain a dissolution vessel temperature of 340-360 K with the wastes that have been considered in these investigations. The heated waste solution was injected into the calciner at a rate of 2-3 l/hr with preheated air or an inert gas

ORNL-DWG 80-11383RC0

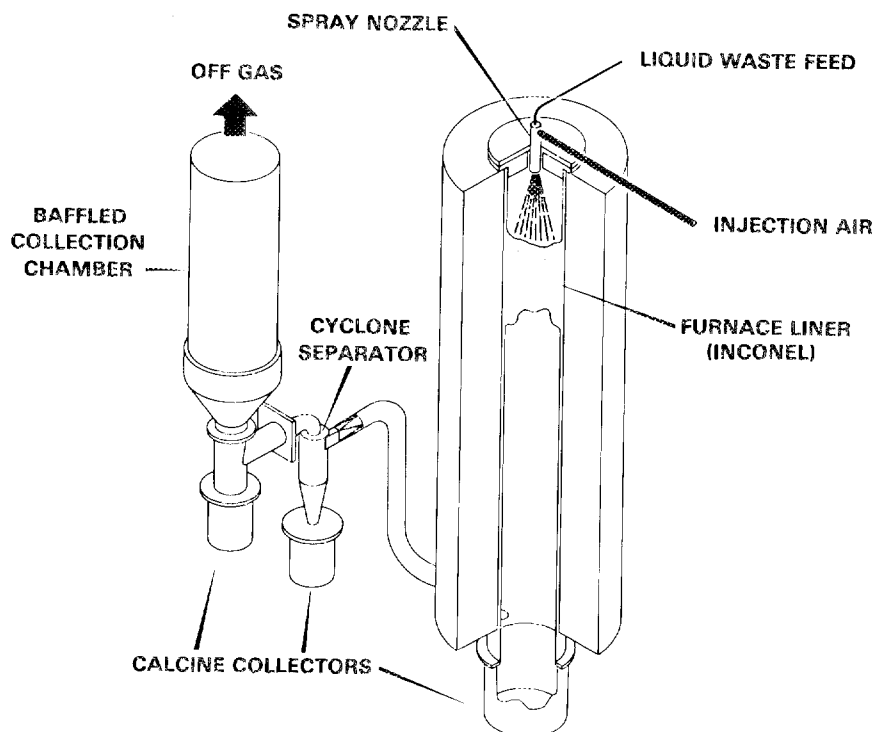


Fig. 5. Schematic diagram of the reactive spray calciner including one of the optional methods for calcine collection.

using the spray nozzle shown in Fig. 6. This nozzle was designed to provide effective atomization of the molten urea solution and produce the narrow spray pattern shown in Fig. 7. The injection gas flow rates for this nozzle were typically 3-5 cubic feet per minute at 770 K. A balance in droplet size produced by the nozzle had to be achieved to provide maximum droplet sizes and subsequent particle sizes for ease of collection while maintaining a small enough droplet to permit complete and rapid calcination. The droplet size is a function of the nozzle design and the physical properties of the feed solution. A typical feed solution with a density of 1.33 g/cc was shown to have a viscosity of 0.75 mPa • s at 333 K and a surface tension of 7.6×10^{-3} N/m at 347 K. These properties coupled with the existing feed stream and injection gas flow rate ranges

ORNL-DWG 79-20814

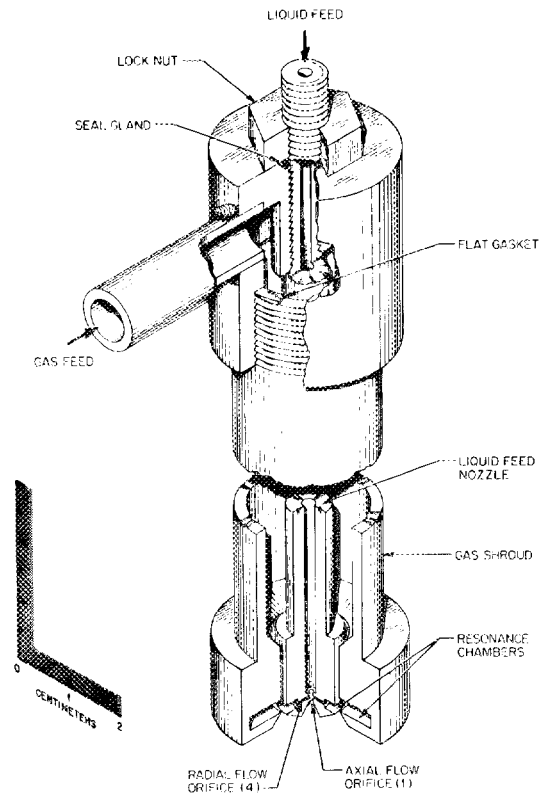


Fig. 6. Schematic representation of the nozzle used for the spray calcination of molten urea solutions.

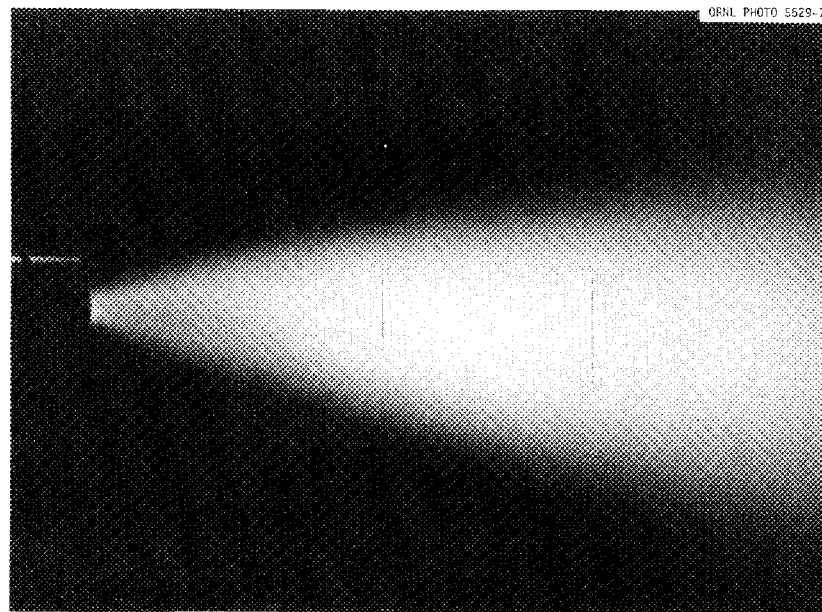


Fig. 7. The narrow, well atomized spray pattern provided by the nozzle (Fig. 6) permits effective calcination of molten urea solutions.

yielded calculated droplet sizes of 8-56 μm . When calcined, this range of droplet sizes produced particles with measured diameters ranging from 0.3 μm to agglomerates exceeding 500 μm . The size distribution of calcine particles produced with a waste stream feed rate of 2.3 l/min and an injection gas flow rate of 3.7 cubic feet per minute at 770 K is shown in Table 3.

In the tests that were conducted with the reactive spray calciner, wall temperatures were initially maintained at 1270 K and successively reduced to 1070 K in later tests. In all cases, centerline temperatures were maintained at or slightly below the wall temperature by the exothermic heat of the calcination reactions. Although a wall temperature of 1070 K was the lowest operating temperature tested, it is felt that satisfactory calcination may be achieved at lower temperatures since these exothermic reactions, once initiated, may be able to provide sufficient heat to the particles to produce complete calcination. Throughout the temperature range tested, no build-up of material on the calciner walls was observed. Tests of calcine powder showing the absence of residual nitrates in the powder and an equilibrium pH of 6.5 for calcine slurried in water are further indications of the successful calcination of waste and additives in molten urea solutions using the reactive spray calcination process.

After calcination, the next major task to be performed was the separation of the powder from the off-gas and its collection. The calcine collection system, shown in Fig. 5, provided for the separation of greater than 98% of the material with less than 2% escaping the unfiltered collection system as fines requiring filtering or some other final separation process. The coarse particles and agglomerates are collected in the pot

Table 3. Typical Calcine Particle Size Distribution

<u>Size Microns*</u>	<u>Wt. %</u>
+500	2.4
+300	0.6
+212	4.3
+180	2.9
+150	6.5
+90	16.3
+63	25.1
+45	18.1
-45 ⁺	23.7

* Particles +500 μm were agglomerates of smaller particles.

+ Minimum-sized particles observed were 0.3 μm .

at the bottom of the calciner body. Finer particles are carried in the off-gas stream and enter the cyclone separator at a velocity of 6-21 m/s. The cyclone separator was designed to remove particles with diameters of 5 μm and larger from gas streams in this velocity range. The off-gas is next routed to a baffled collection or settling chamber where its velocity is reduced to less than 1.5 m/s. It was in this chamber that the magnetic properties of the calcine powder were used to advantage to improve the separation of the remaining fines from the off-gas. Various magnetically enhanced separation techniques were being investigated to optimize the separation of solids from the off-gas, thereby simplifying subsequent off-gas handling requirements. Finally, it was found that through control of the off-gas temperature in the system, water vapor could be condensed at

a desired location, for example, in the settling chamber. This condensed water vapor effectively "scrubbed" the off-gas, removing a considerable amount of the fines that escaped separation in the preceding step(s).

Examples of the calcine particles are shown in Fig. 8. As evidenced by the ductility of the mechanically deformed particle shown in the higher magnification micrograph, the use of an inert injection gas results in partial, if not complete, reduction of the metal species in the waste. Although no radiotracer volatility tests could be performed on the reactive spray calciner because of radioactivity limitations of the facility, there are strong indications that the low radioisotope volatility losses observed in batch processing (discussed in a later section) would be lower using the reactive spray calcination process with either an inert gas or air for the injection of the waste stream into the calciner as compared to the batch process (described above).

Cermet Densification Methods

Significant changes and improvements have been made in the flowsheet regarding the densification process. Initially, calcine powder, in the form of mixed oxide, was reduced to yield a mixed metal-oxide powder. A "green" compact was formed by mixing this material with a wax binder and subjecting the mixture to cold compaction by pressing or extrusion. Subsequently, the green compact was sintered at temperatures from 1470 to 1670 K in a non-oxidizing atmosphere. Slow initial heating of the green compact was required to permit quiescent volatilization and removal of the wax binder without distortion of the cermet body. The sintering cycle continued beyond this point with a heating rate of 100 K/hr up to the desired temperature, which was typically maintained for 10-12 hours

ORNL-PHOTO 4468-81

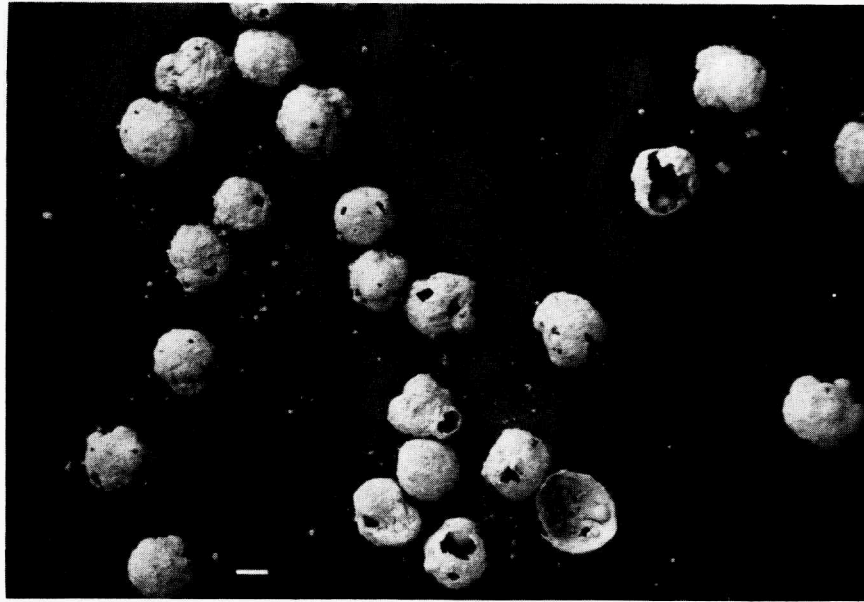


Fig. 8. (a) SEM micrograph of typical calcine particles.

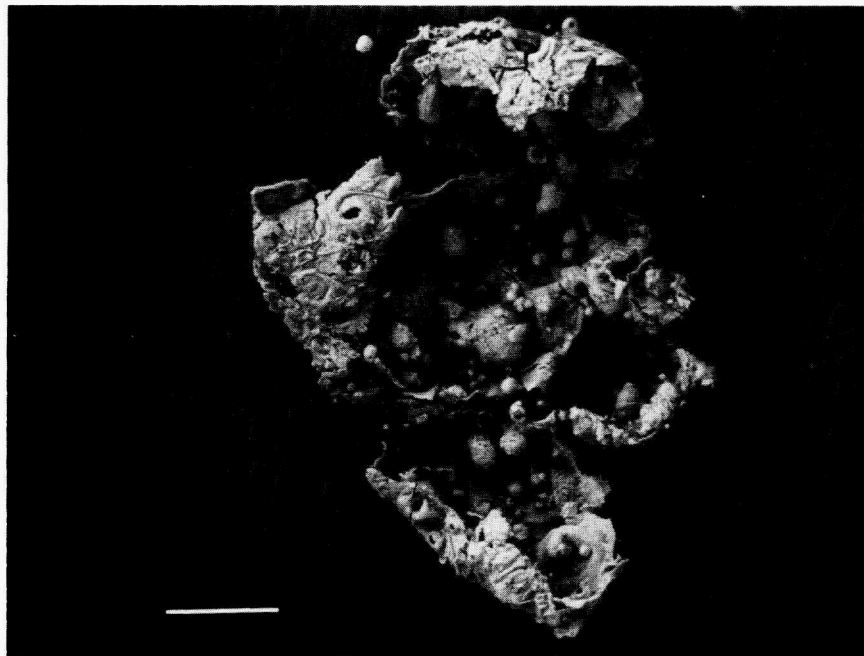


Fig. 8. (b) Reactive spray calcination using an inert injection gas results in partial, if not complete, reduction of metal species as indicated by the ductility of this mechanically deformed particle (bar length represents 50 μm).

followed by furnace cooling. In total, this sintering cycle required at least 24 hours to complete.

Alternatively, reduced calcine powder was loaded into a graphite die and vacuum hot pressed to yield a dense cermet body. Hot pressing was typically performed at a pressure of 27.6 MPa (4000 psi) at temperatures ranging from 1320-1420 K. It was found that hot pressing at higher temperatures produced a laminar microstructure with alternating metal and ceramic-rich layers. This nonuniform distribution of the ceramic particles in the metal matrix is not desirable in that microencapsulation of the ceramic particles and the thermal conductivity of the bulk cermet body are degraded. Because hot pressing techniques applicable to remote processing are complex and essentially batch type, especially on the large scale required for waste applications, hot pressing is considered feasible only for fabrication of base-line samples against which cermets produced by other densification techniques can be compared.

Similar to improvements made in the chemical processing portion of the flowsheet, densification developments should simplify the process and be compatible with engineering scale-up. One of the first important improvements was the substitution of water for the wax binder when cold compaction of the calcine was performed. Water lends satisfactory strength to the cold compact and provides sufficient lubrication necessary for cold-forming while being much easier to remove from the resultant compact. Use of water as a binder eliminates the need for carefully controlled, slow heating in the sintering cycle; the process can be carried out more rapidly, and the porosity of the product cermet is significantly reduced.

Combination of the reduction and sintering processes into one operation was performed successfully. A cold compact of the calcine oxide powder was formed and sintered in a reducing atmosphere which reduced appropriate cations to metals forming the alloy matrix; as the temperature increased, the cermet body densified by conventional sintering.

An alternative, low-temperature method for densification was investigated briefly. In this case, the calcine oxide powder was reduced at approximately 1070 K in an atmosphere containing hydrogen or carbon monoxide and subsequently compacted by cold isostatic pressing. The fine metal particles in the reduced powder were effectively cold-welded to yield a strong, dense cermet body. It remains to be determined whether subsequent heat treatment of this compact is required to improve the quality of this cold-compacted cermet. For this method of densification, a reduced calcine powder is required as the starting material, and, as mentioned previously, operation of the spray calciner as a closed system can result in such a reduced calcine powder suitable for isostatic pressing without further treatment. A major concern associated with this densification method is whether the desired ceramic phases are suitably formed at the reduced process temperature. It is expected that the exothermic urea-nitrate reaction would heat the individual powder particles to temperatures well beyond the 1070 K calciner wall temperature and thus the formation of the desired ceramic phases should occur. Proof of attainment of suitable ceramic phases and the determination of whether heat treatment subsequent to isostatic pressing is required and are the key factors determining the acceptability of this densification process. If this method is determined to be suitable, significant reduction of processing temperatures could

result with associated elimination of more complex, high temperature, in-cell processing.

Finally, a new sintering technique was demonstrated (but requires further development) which would permit simultaneous sintering and reduction at significantly reduced times and temperatures than those required for conventional sintering [7]. This technique relies on the formation of small amounts of liquid in the compact during reduction at elevated temperatures; enhancement of densification occurs through liquid phase sintering mechanisms [8].

Initially, the oxide calcine was either reduced prior to compaction and sintering, or reduced during the sintering cycle by holding the material at 1070 K in a reducing atmosphere for several hours during the heat-up schedule. These conditions do not result in the formation of a liquid phase, and densification with a subsequent conventional sintering cycle required approximately 24 hours. The thermal cycle consisted of a 100 K/hr heat-up to 1073 K, a several hour soak at 1073 K to assure full conversion of reducible metal oxides to metal followed by 100 K/hr heating to the final sintering temperature; sintering continued for up to 8 hours before cooling.

Tests of an alternative thermal cycle have shown that satisfactory densification of cermets (with low porosity) can be achieved at temperatures as low as 1320-1370 K in as short a period as 20 minutes. It has been found that if a compacted calcine body is heated up very rapidly in a reducing atmosphere, a liquid is generated by the elevated temperature reduction of metal oxides to metal (and suboxides). This thermal and chemical process is shown schematically in Fig. 9 along with

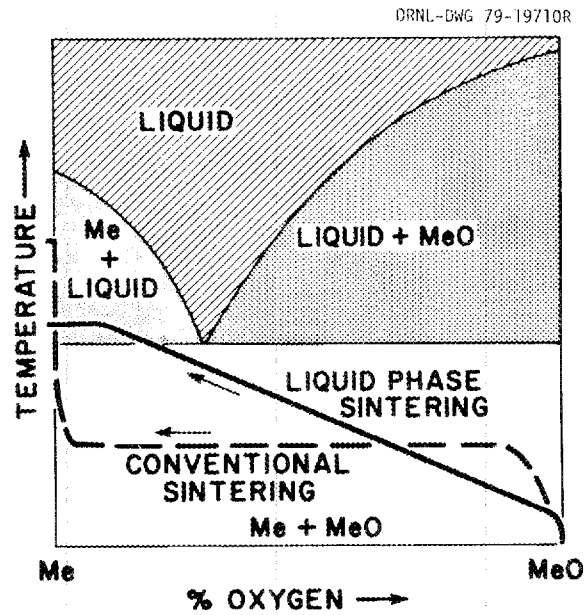


Fig. 9. Schematic illustration of mechanism for liquid phase sintering of cermets.

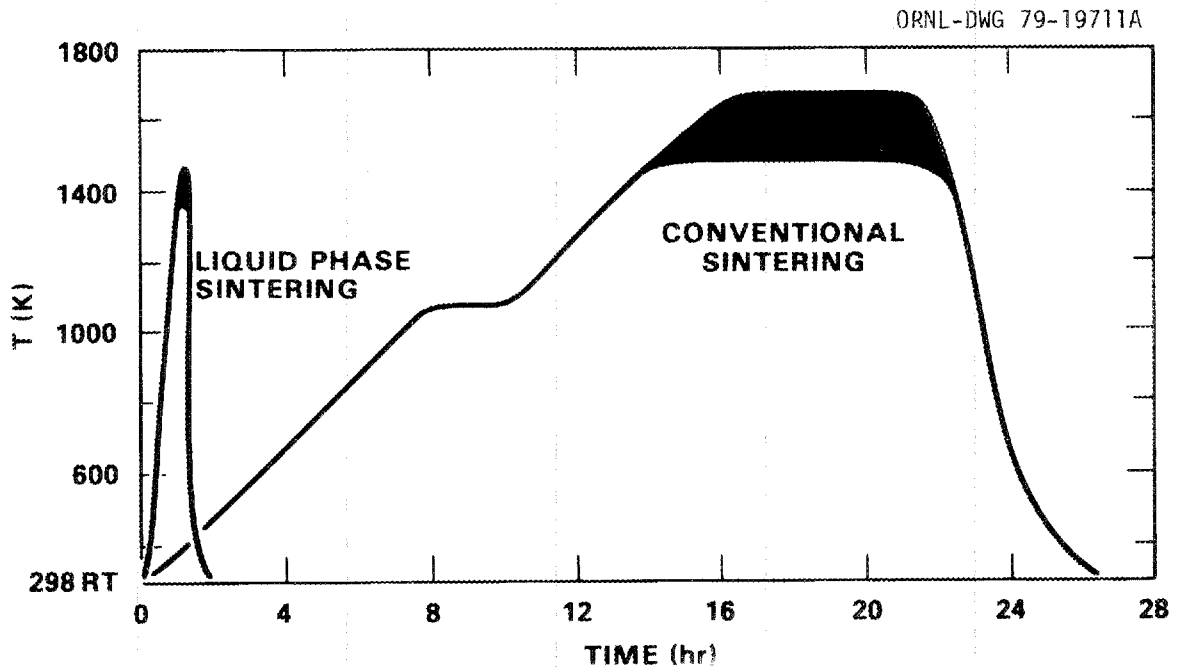
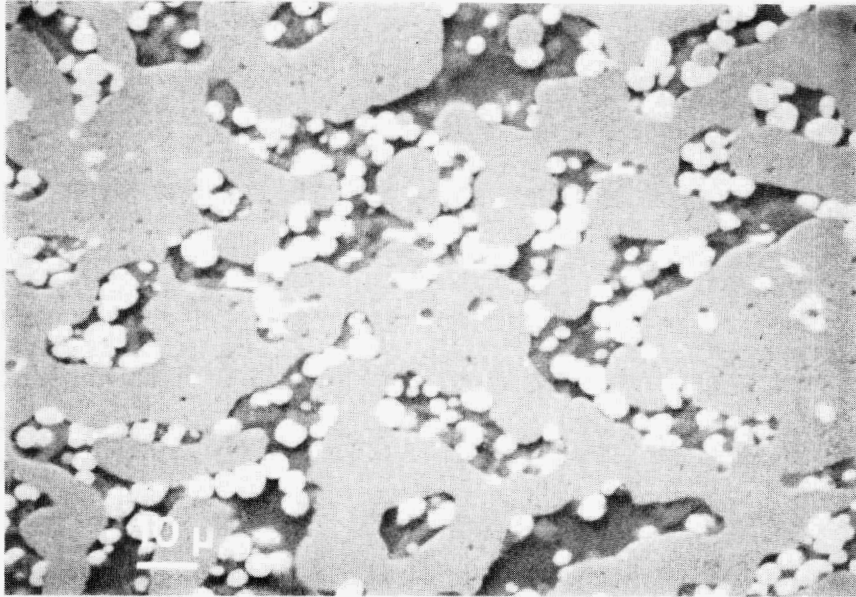


Fig. 10. Typical temperature-time profiles for conventional and liquid phase sintering show some of the advantages of the latter.

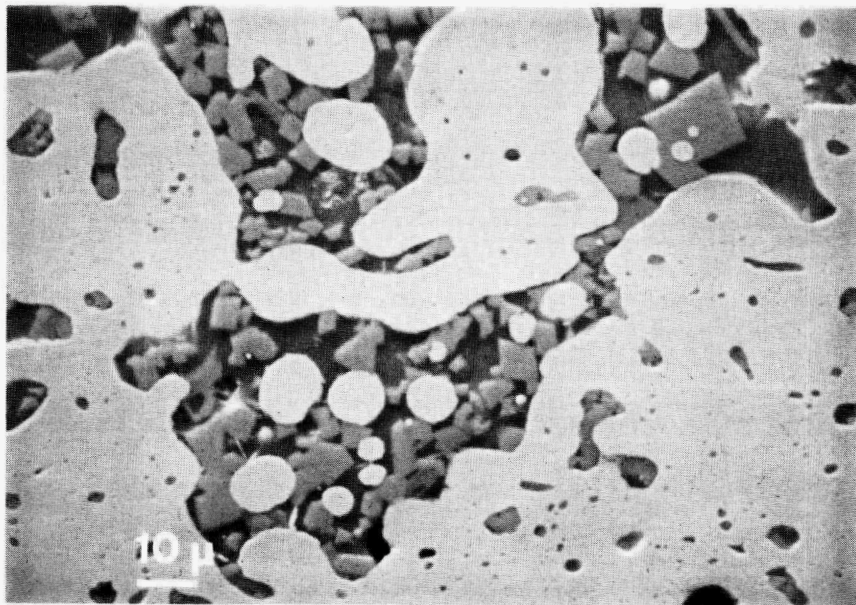
the time-temperature comparative profiles for the two sintering methods in Fig. 10. A comparison of the cermet microstructures generated by liquid phase sintering versus conventional sintering can be seen in Fig. 11. The micrograph in Fig. 11(a) illustrates the results of conventional sintering of a sample of actual NFS Acid Thorex waste. Rounded ceramic particles, composed primarily of ThO_2 , are dispersed throughout the metal matrix but tend to be located in microporosity and are less than satisfactorily microencapsulated by the metal matrix. In contrast, the micrograph in Fig. 11(b) illustrates the improved microencapsulation and densification achieved by the liquid phase sintering process. This particular sample was prepared from actual, fresh SRP acid waste. Further refinement of processing parameters is required before this new sintering technique becomes a standard practice for cermet densification. When developed, the liquid phase sintering technique will not only significantly reduce the time required for densification, but also will lower process temperature requirements.

Summary

In summary, a variety of alternate unit operations have been studied and partially developed which would simplify the process flowsheet, reduce processing temperatures and shorten processing times without compromising the quality of the final cermet. In many cases, improvement of the properties of the final cermet body resulted. Remote handling, maintenance, safety and economic considerations of these processing techniques were evaluated on a preliminary basis. A variety of engineering evaluations of these relatively new waste processing methods have been carried out at other DOE sites.



(a)



(b)

Fig. 11. Comparison of microstructures of actual waste cermet samples prepared by different sintering techniques.

- (a) NFS Acid Thorex Waste - conventional sintering
- (b) SRP Acid Waste - liquid phase sintering

VOLATILITY LOSS STUDIES

A major concern during processing of high-level radioactive wastes into cermet or any other solid storable form is the volatilization of radioisotopes contained in the waste. Volatility loss data have been determined for Cs, Ru and Sr in radiotracer cermet processing tests and for Cs and Ru in actual waste processing tests. Data were obtained from analyses of solution samples taken from three-column scrubbers through which all processing off-gases were passed. These volatility losses were determined for the small laboratory-scale cermet process beginning with the urea precipitation step through the sintering operation. Fig. 12 shows a scrubber attached to the calciner furnace that was installed in a hot cell for the actual waste experiments. The fitting in the lower right corner was connected to the cell off-gas system to provide constant suction during processing and to minimize contamination of the cell by entrained powder and/or gaseous products. A smaller scrubber was used for radiotracer volatility studies. In both cases, the scrubbers were first attached to the precipitation vessel, sampled and flushed; then attached to the calcining furnace, sampled and flushed again; and finally attached to the sintering furnace. Data obtained from these scrubber experiments represent maximum losses which may overstate the actual losses caused by volatilization. It was neither practical nor desirable to install particulate filters between the processing equipment and the off-gas scrubbers; therefore, fine particles could be entrained in the off-gas and transported to the scrubbers. Entrainment would increase the concentration of radioactive species in the scrubber samples and reflect a higher volatility loss than had actually occurred.

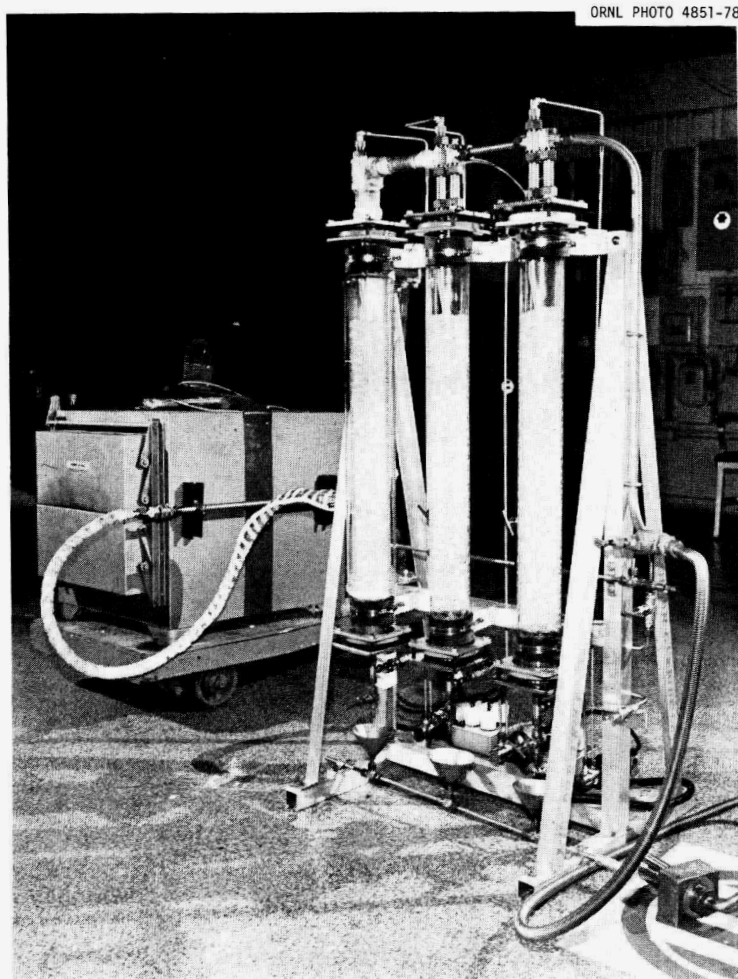


Fig. 12. Scrubber columns attached to calcination furnace which were installed in a hot cell for actual waste volatility studies.

In the radiotracer volatility experiments, losses during the precipitation and calcination steps were found to be 0.014% Cs, 0.18% Ru and 0.0001% Sr. During sintering, these losses totaled 0.0023% for Cs, 0.055% for Ru and 0.000006% for Sr. Total maximum volatility losses during the entire process are the sums of these two sets of data, i.e., 0.016% Cs, 0.23% Ru and 0.0001% Sr. Smearing for radioactivity in the manifold between the processing equipment and the scrubber system showed negligible surface activity, thus providing corroboration that the observed

results were probably representative of volatility losses and that radioactive species had not condensed in the manifold. These results represent very low process volatility losses.

Unfortunately, failure of the hot cell off-gas system that powered the scrubbers prevented acquiring volatility loss data during processing of actual NFS acid Thorex waste. However, data from processing actual untreated SRP acid waste were obtained. These data are shown in Table 4. Although these results differ slightly from those obtained during radiotracer tests, they too represent very low volatility losses during cermet processing. Since the samples in this latter test were drawn from the scrubber columns in the cell, the possibility of external contamination of these samples exists, which, along with possible particle entrainment effects, would exaggerate the true volatility losses.

Limited tests were conducted to determine the volatility losses of technetium during processing. Using the batch process steps of precipitation calcination, reduction and sintering in a reducing atmosphere, approximately half of the technetium in the simulated waste samples was volatilized. The calcination step, which consists of a several hour exposure to air at elevated temperatures, was primarily responsible for these high losses. It is felt that the use of reactive spray calcination rather than batch precipitation and calcination would significantly reduce the volatilization of technetium since exposure times to high temperatures in combination with an oxidizing atmosphere would be reduced or eliminated. Again, because of radioactivity limits on the spray calciner facility, the behavior of technetium during spray calcination could not be evaluated.

Table 4. Volatility Losses of Cs and Ru during Processing of Fresh SRP Acid Waste

	<u>Precipitation</u>	<u>Calcination</u>	<u>Sintering</u>	<u>Total</u>
Cs (% Lost)	0.0029	0.1006	0.1653	0.2688
Ru (% Lost)	0.0022	0.0007	0.0004	0.0033

In summary, radioisotope volatility data clearly show that very low losses occur during processing of wastes to cermet form. The low volatility losses experienced in the cermet process are attributed to two different factors. First, urea provides a basic, chemically reducing environment which maintains elements such as ruthenium, in a nonvolatile state (elemental or dioxide). Second, formation of specific ceramic mineral phases effectively traps specific nuclides in low vapor pressure forms--cesium as pollucite and strontium as titanate. Because volatility losses during cermet processing appear quite low, minimal demands on an off-gas handling system should result for cermet processing and the generation of additional wastes requiring subsequent treatment could be much less than for other waste form preparative processes.

CERMET LEACHABILITY

One of the primary requirements placed upon a solid high-level waste form is its resistance to leaching of the various contained radioactive species under a variety of conditions likely to be encountered during transportation and storage. Cermet is designed to meet this requirement at two levels. First, the cermet form is made to fix leachable species in the forms of stable insoluble crystalline ceramics such as oxides, aluminosilicates and titanates. A second level of fixation is provided by the alloy

matrix, which essentially microencapsulates the multimicron size ceramic particles and which itself contains some radioisotope species, such as, Ru, Co, etc. Additions, when required to supplement quantities of materials already in the waste, are made so as to formulate the desired chemical compositions of the ceramic phases and the alloy matrix. These additions are made in the urea dissolution process at the head end of the flowsheet.

While much of the ceramic portion of the cermet consists of oxides, additions are made to permit the formation of aluminosilicates, such as pollucite for cesium fixation, and titanates for strontium fixation. Generally, these additions are made in amounts which when summed with those elements already in the waste yield a 50% excess of the amount required to compound the fission products. Although not a fission product, the highly leachable sodium content of the waste must be isolated in a leach resistant ceramic phase, i.e., an aluminosilicate, to preserve the physical integrity of the cermet body in contact with a leachant.

The alloy matrix of cermets is primarily derived from reducible metal species present in the waste with minor additions to formulate an alloy having high corrosion resistance. While extensive studies have not been undertaken to optimize the alloy matrix composition, an alloy having 70 wt. % Fe, 20 wt. % Ni, 5 wt. % Cu and 5 wt. % miscellaneous metals was used primarily. This formulation is considered to be a typical composition based on metal species occurring in a variety of wastes and the general economic availability of alloying additives. Cermets having an essentially pure nickel matrix and a 50 wt. % Fe - 50 wt. % Ni matrix have been prepared. The matrix can be composed of any metal or alloy, which is reducible under the particular processing parameters used, for

optimum performance during transportation and disposal. This matrix will, however, also contain those inert and fission product cations already in the waste that are reducible.

Qualitative and quantitative leach testing of cermets under a variety of conditions have been performed at ORNL and Battelle Pacific Northwest Laboratory (PNL). Experimental difficulties were encountered in some of these tests, and therefore, available leach data is only of a preliminary nature. A program for quantitative leach testing of cermets was being formulated which should have eliminated the difficulties experienced in tests at ORNL and PNL; however, it was not implemented because of the termination of the program. This program included the testing of a variety of simulated wastes (with and without radiotracers) and samples of actual high-level wastes which have been converted to the cermet form. Preliminary leach behavior of cermets, as summarized below, was to have been quantified and the cermet leaching mechanisms delineated.

As reported previously [1], early qualitative leach tests were performed on a simulated SRP waste hot-pressed pellet and an extruded-sintered rod. Both samples were exposed to boiling, saturated NaCl solutions for 168 hours at atmospheric pressure. Mass spectrographic analyses of the leachant showed no detectable leaching of the cermet samples; the only ionic species observed to increase in the leachant were silicon and boron, presumably from the Pyrex beakers used in the tests. No corrosive attack of the extruded-sintered rod was visible and only spotty discolorations were observed on hot-pressed samples, which were attributed to surface carbide that had formed during hot-pressing in a graphite die.

A qualitative autoclave test was performed on a hot-pressed pellet containing simulated SRP waste having a high manganese oxide content.

After four days at 490 K and 2.1 MPa in the standard Waste Isolation Pilot Plant (WIPP) "B" brine solution, slight surface attack resembling a tarnish was visible. Mass spectrographic analysis of the leachant showed that the manganese oxide in the cermet was being preferentially attacked to a small degree. This was supported by optical and SEM/XES metallographic analyses showing attack of the manganese oxide particles on the surface of the pellet. No attack of the metal phase or other ceramic phases was detectable either by mass spectrographic or metallographic analyses.

A series of radiotracer-containing cermet samples were prepared from simulated NFS acid Thorex waste in an attempt to determine quantitative leach rates for these cermets in distilled water and brines. Each sample contained tracer quantities of ^{137}Cs , ^{89}Sr , ^{106}Ru or ^{60}Co . The ^{137}Cs and ^{89}Sr tracers were used to monitor their respective ceramic phase leach behavior while the ^{106}Ru and ^{60}Co were used to provide data on the behavior of the alloy matrix during leaching.

The apparatus used in these leach tests, shown in Fig. 13, was designed to test cermet pellets in distilled water or a variety of brines at temperatures up to the leachant boiling point at atmospheric pressure. The leachant was circulated around the submerged pellet by the percolator as shown in Fig. 14.

This first series of cermet leach tests, conducted at ORNL, was subject to experimental difficulties which compromised the validity of the resulting data. Among the problems experienced in this test series were evaporative losses which subsequently required repetitive additions of makeup water. Secondly, the vibrating action of the pellets caused by percolation of the leachants resulted in minor abrasion of material from

the samples. Finally, analytical results obtained from counting the leachant samples were found to be inconsistent. In some cases, these inconsistencies appeared to be related to the analytical technique itself while others were attributed to leachate sampling methods and sample storage.

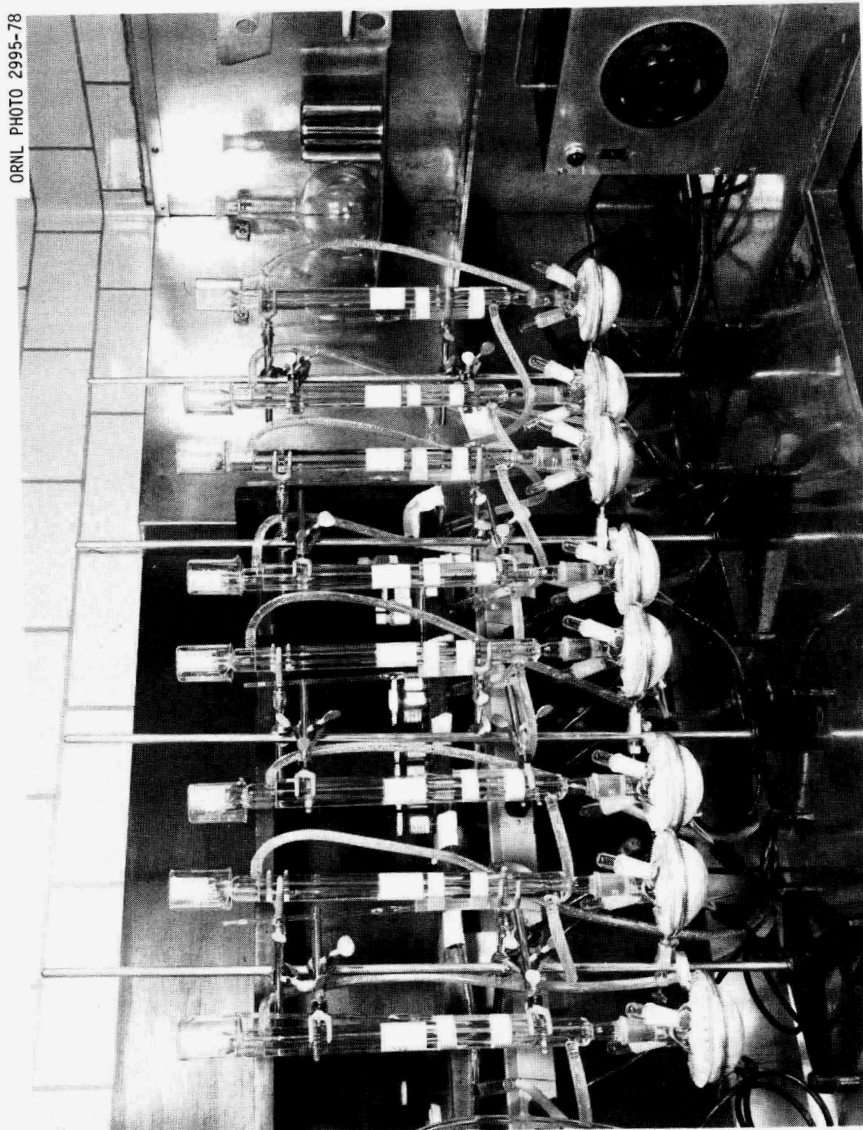


Fig. 13. Leaching apparatus for early radiotracer leach tests at ORNL.

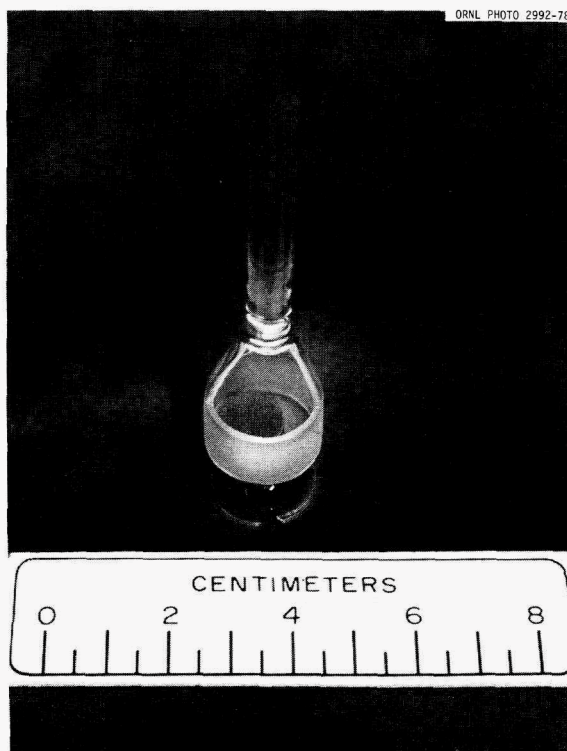


Fig. 14. Percolator used for leachant circulation in early radiotracer leach tests at ORNL. Resulting abrasion of sample surface proved unsatisfactory.

A second set of cermet samples was prepared from simulated NFS acid Thorex waste; each sample contained ^{137}Cs and ^{106}Ru radiotracers. These samples were sent to PNL for leach testing. These cermets were composed of 37 wt. % mixed ceramic phase and 67 wt. % metal alloy matrix having a nominal composition of 70% Fe-20% Ni-5% Cu-5% Co on a weight basis. One cermet sample was used in each of the following tests:

- a) 72 hour, Soxhlet test;
- b) 31 hour, 298 K, pH 4 acetate buffer test;
- c) 31 hour, 298 K, pH 9 ammonium hydroxide-HCl buffer test;
- d) long-term modified IAEA leach test at 298 K in distilled water with decreasing sampling frequencies;

- e) 7 day, 620 K, 16.5 MPa distilled water autoclave test; and
- f) 7 day, 620 K, 10.7 MPa, saturated brine autoclave test.

Unfortunately, in all but the Soxhlet test and late stages of the long-term, modified IAEA test, cermet samples were placed in direct contact with various metals in the test apparatus, resulting in galvanic coupling. The role of galvanic coupling in these tests and its affect on the resulting data have not been fully determined. Leach rates were calculated from dry weight changes and radioisotope analyses of the leachant, using the geometrical surface areas of the cermet samples, as shown below:

$$\frac{(W_o - W)}{SA \times T} = g/cm^2 \cdot d^* \quad (\text{weight basis})$$

$$W_o \left(\frac{A}{A_o} \right) \div (SA \times T) = g/cm^2 \cdot d \quad (\text{isotopic basis})$$

A_o = original radioisotope activity in samples

A = activity leached

W_o = original dry weight

W = dry weight after test

SA = geometric surface area

T = incremental or total test period in days

*Some samples exhibited a weight gain caused by oxidation of the matrix and deposition of reaction products as caused by galvanic coupling. This mathematical expression was not applicable in these situations and for similar reasons, was questionable in other tests.

The percentage of each radioisotope tracer released over the duration of the tests was also calculated. While the results of these test calculations may not be comparable to those determined for other waste forms under similar conditions, intercomparison of the cermets leachability under these varied leach conditions would seem to be a valid option.

Results of the Soxhlet, pH 4, and pH 9 tests are shown in Table 5. Of these three tests, only the Soxhlet test was performed in the absence of galvanic coupling. Therefore, this is the only test in the PNL series in which identical test conditions provide a basis for comparison between the cermet waste form and glass waste forms tested at PNL. During Soxhlet leach testing of a 78-68 solid glass sample at PNL, a leach rate of $9 \times 10^{-4} \text{ g/cm}^2 \cdot \text{d}$ was determined as based on weight loss [9]; this value is to be compared with $7.1 \times 10^{-6} \text{ g/cm}^2 \cdot \text{d}$ for the cermet sample. No glass leach data based on cesium or other radiotracer analyses were available from PNL. Therefore, comparison of results from these leach tests is still somewhat ambiguous. The surface appearance of the cermet sample after Soxhlet leach testing is shown in Fig. 15. In both the pH 4 and pH 9 tests, the samples were suspended in buffered leachants in Type 304L stainless steel mesh baskets. Visual examinations revealed obvious galvanic coupling effects as evidenced by a brown stain or reaction product deposition layer on the cermet samples and the mesh baskets at contact areas. The results from the long-term, modified IAEA leach test showed sporadic variations in incremental leach rates of a magnitude of $10^{-6} \text{ g/cm}^2 \cdot \text{d}$ when based on cesium analyses. As noted above, the sample was suspended in the leachant using a Type 304L stainless steel basket which resulted in galvanic coupling. Late in the test, which lasted

Table 5. Results of PNL Leach Tests A, B, C.

	(A) Soxhlet test 72 hour	(B) pH 4 31 hour	(C) pH 9 31 hour
wt. loss basis			
% loss	0.002	0.11	0.0024
$\text{g/cm}^2 \cdot \text{d}$	7.1×10^{-6}	7.4×10^{-4}	1.6×10^{-5}
Cs analysis basis			
% Cs release	0.024	0.072	0.015
$\text{g/cm}^2 \cdot \text{d}$	7.18×10^{-5}	4.75×10^{-4}	2.43×10^{-4}
Ru analysis basis			
% Ru release	N.D.*	0.0016	0.003
$\text{g/cm}^2 \cdot \text{d}$	N.D.	1.02×10^{-5}	1.72×10^{-6}

*N.D. - No Ru detected in leachant.

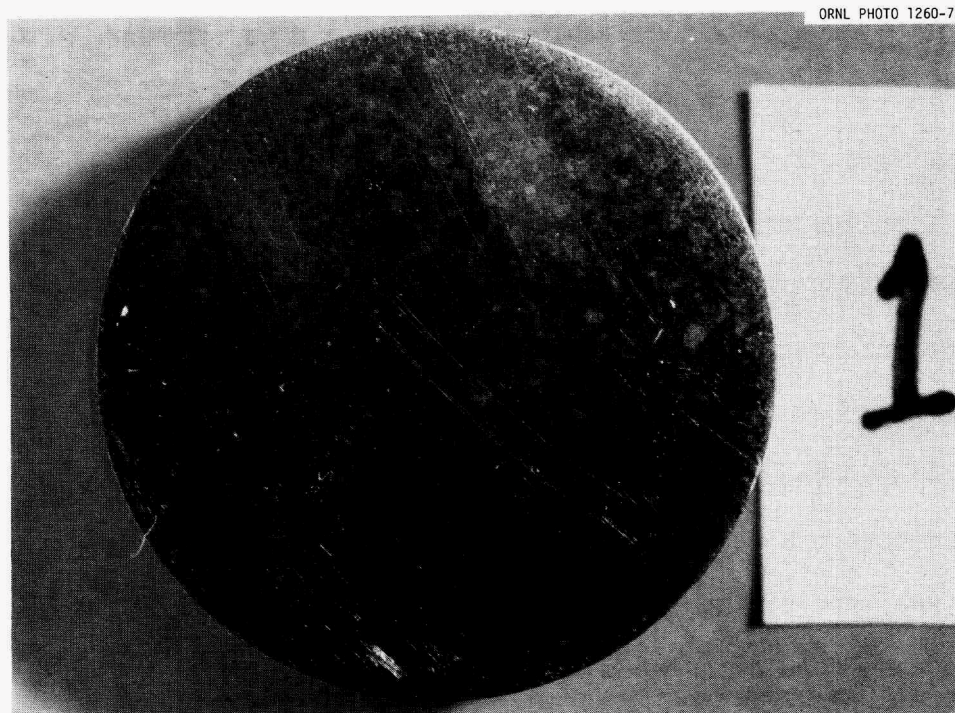


Fig. 15. Macrograph of cermet sample surface following Soxhlet leach testing shows essentially no change in appearance as a result of the test.

146 days, a plastic basket was substituted for the stainless steel basket. Figures 16 and 17 show the sample surface with its surface deposit resulting from galvanic coupling, and the cross sectional area at that surface where some local reaction had occurred. The penetration depths of reaction layers did not exceed five microns and these areas of penetration were evident only at those locations where surface depositions had formed. Because of the sporadic leach behavior, testing complications and the lack of repetitive tests for comparative purposes, no conclusion is drawn from this test regarding the extended-term leach behavior of cermets.

Two high-pressure, elevated-temperature autoclave leach tests (e, f) were performed at PNL on radiotracer-containing cermet samples. One sample was exposed to distilled water for seven days at 620 K and 16.5 MPa while the other sample was tested in saturated brine for seven days at 620 K and approximately 10.7 MPa. Galvanic coupling again was present in these tests since the samples were held in Inconel 600 beakers inside Hastalloy "C" autoclaves. In the distilled water test, a weight gain of 0.0025% was observed, while analysis of the clear leachant showed a cesium release of 12% corresponding to a calculated leach rate of $1.5 \times 10^{-2} \text{ g/cm}^2 \cdot \text{d}$. A gray adherent coating or tarnish formed on the cermet in this test; however, no local attack or pitting was apparent by visual examination. The sample exposed to hydrothermal conditions in saturated brine developed a thicker, black, adherent coating and showed a weight gain of 2.82%. Analysis of the leachant indicated a 38% Cesium release, corresponding to a calculated leach rate of $3.9 \times 10^{-2} \text{ g/cm}^2 \cdot \text{d}$. In both tests, the cermet samples totally maintained their physical integrity.

Metallographic examinations of these samples confirmed that formation of layers on the surfaces of these samples, as illustrated in Fig. 18, had occurred with the layer formed during the brine test being thicker than that formed in the distilled water test. A few cracks up to approximately 100 μm in depth were observed; however, it is unclear whether these cracks formed as a result of the hydrothermal test conditions or as a consequence (more likely) of the preparative methods employed for these samples. Deposits of an iron-containing corrosion product were observed at various locations within these cracks. The presence of other alloying elements in these deposits were not detected. Finally, in spite of the apparently large cesium releases indicated by leachant analyses (12% and 38%), no significant depletions in cesium content of the surface or near surface aluminosilicate particles was found as determined by energy dispersive x-ray analyses.

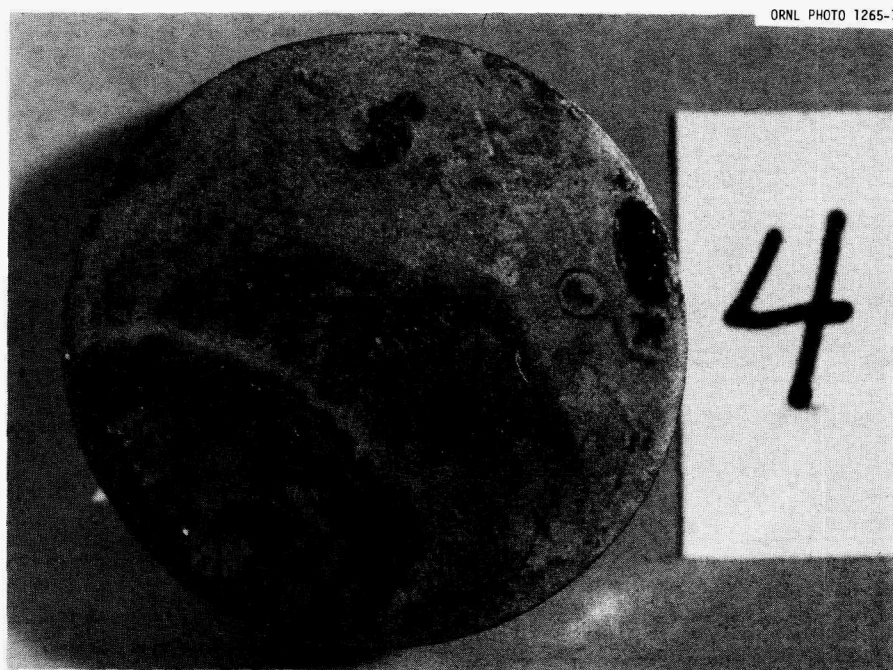


Fig. 16. Macrograph of cermet sample surface following 146-day leach test. Apparent galvanic coupling with stainless steel mesh basket resulted in surface deposits on the cermet sample.

ORNL-PHOTO 4470-81

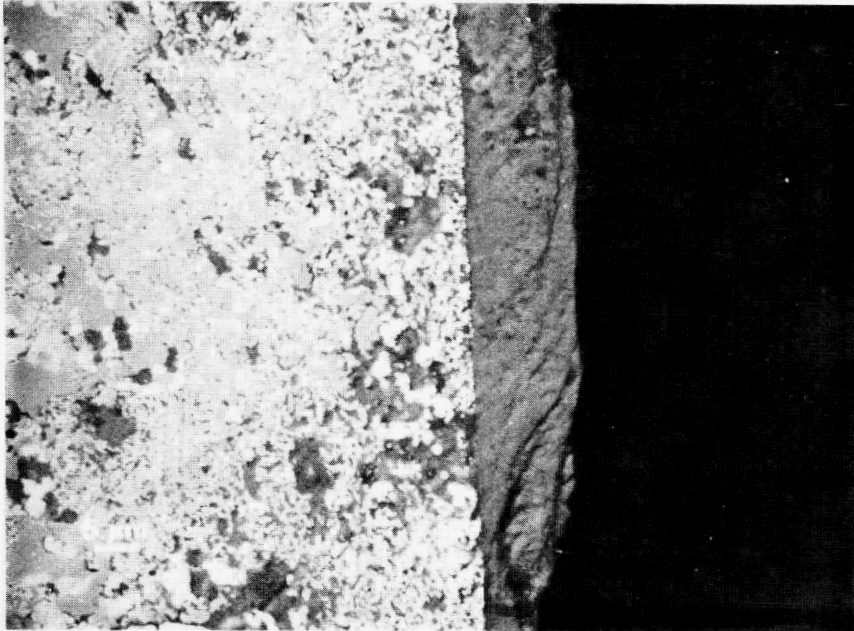


Fig. 17. SEM micrograph of the cross section of the 146-day leach test sample shows minimal attack of cermet, even in areas where deposits of "rust" occurred as a result of apparent galvanic coupling.

ORNL-PHOTO 4471-81

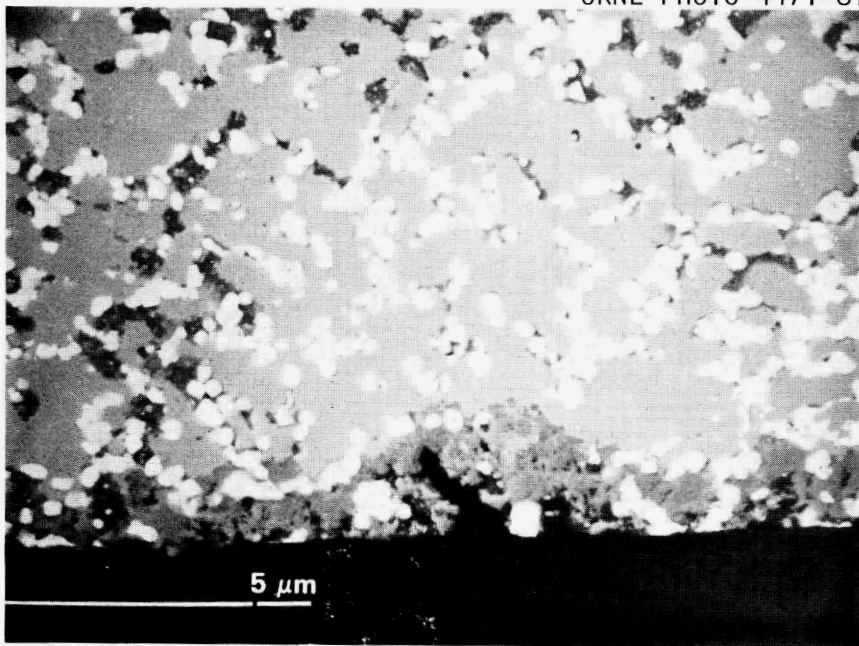


Fig. 18. SEM micrograph of the cross section of the hydrothermal brine leach test sample showing the thin, adherent reaction layer which developed on the cermet surface.

The corrosion resistance of the metal matrix can be enhanced first, by compositional selection and control and secondly, by simple application of galvanic coupling principles. The galvanic series shown in Table 6 gives the ranking of degree of nobility of two cermet alloy formulations relative to a variety of metals in WIPP "B" salt solutions. The selection of a corrosion resistant metal to be in contact with the cermet waste form, as part of the containment package, that is also anodic with respect to the cermet matrix, could significantly delay any corrosion of the matrix metal that might otherwise occur in a particular environment.

Table 6. Preliminary Galvanic Series Results in WIPP "B" Solution

	<u>Material</u>	<u>Potential (V) vs. Pt</u>
Noble or	Pt	-
Cathodic	Ti	-0.190
	304 SS*	-0.350 (passive)
		-0.500 (active)
	Cermet (50 Fe-50 Ni)	-0.580
	Cu	-0.600
	Cermet (70 Fe-20 Ni- 5 Cu-5 Misc.)	-0.720
	Pb	-0.860
Active or	Zn	-1.375
Anodic		

*304 stainless occasionally suddenly becomes activated after which there is an exponential decay to the passive potential.

It is clear from these results that the leach rate of cermets is very low, but for more quantitative results, more refined leach testing of cermets would be required. Concerns have been expressed that the alloy matrix composition is relatively uncontrolled with probable formation of local corrosion cells leading to the rapid dissolution of the matrix with subsequent rapid leaching and dispersion of the ceramic phases in the cermet [10]. In response to these concerns, it should be noted that the metal matrix can be both controlled and tailored to provide optimum performance for particular disposal environments. There is no experimental evidence to indicate that the compositional homogeneity provided by the urea dissolution process is altered during subsequent processing to the extent that local corrosion cells will develop and hasten the degradation of the cermet waste forms. Finally, in tests where corrosion of the metal matrix did occur, an adherent oxide coating developed which maintained the isolation of the ceramic phase particles and prevented the rapid leaching and dispersion of these ceramic particles.

PROCESSING CHARACTERISTICS AND VARIOUS CERMET PROPERTIES

Those processing characteristics and cermet properties which have not been discussed in separate detail are summarized below.

Waste Loading

The waste loading levels for cermets can vary over a wide range from 2-75 wt. %. In general, as the sodium content of the waste increases, the waste loading decreases since greater amounts of ceramic-forming additives are required to compound and fix the sodium ions. Less waste, therefore,

can be accommodated in this case if the desired ceramic-to-metal ratio in the cermet is preserved. Conversely, as the reducible metal content of the waste increases, waste loading levels can be increased, since this metal in the waste is incorporated in the metal matrix during processing. The sodium and metal contents of the waste have the most significant effect on the maximum waste loading level, aside from possible heat generation or radiation limits being placed on waste packages.

Waste Volume Reduction

The volume of waste, as it is now stored, can be reduced significantly during its conversion to the final cermet storage form. This volume reduction relies mainly on the waste loading level and density of the cermets, which are both relatively high. In converting the waste as dry calcine to the final cermet host, waste volume reduction factors of from 1:1 to 100:1 have been demonstrated.

Metal-to-Ceramic Ratios

No single ratio of metal phase to ceramic phase can be considered optimum since property requirements vary with the different wastes being treated and the subsequent disposal options. Cermets with metal phase loadings from 50 to 80 wt. % metal (balance is mixed ceramics) have been investigated. The metal-to-ceramic ratio must be chosen by considering, among other things, the metal content of the waste and availability of additives, desired thermal and mechanical properties, and various physical properties that are deemed to be of importance to the performance of the overall waste disposal system.

Density

The density of cermets is determined by the formulation chosen for a particular application and the effectiveness of the densification process. Over a wide range of formulations and densification methods, cermet densities have been found to range between 6.0 and 8.2 g/cc. The density, as may be affected by porosity, plays a significant role in determining other cermet properties, i.e., leach resistance, thermal conductivity, etc.

Thermal Conductivity

Measurements on both simulated and real waste cermets with different formulations and densities, have yielded thermal conductivity values between 3 and 20 W/mK with a value of 15 W/mK being typical. In general, as the density or the relative metal phase content is increased, the thermal conductivity of the cermet is increased.

Decay Heat Loading

No limit for decay heat loading has been determined for cermets. Due to the high thermal conductivity of cermets, the internal temperature gradient caused by decay heat is minimal. It is likely that the decay heat limit for the waste storage system will override any limitation imposed by the cermet waste form itself. During very limited testing with actual high-level wastes, samples were prepared having decay heat loadings of 0.02 and 0.2 W/cc for NFS acid Thorex and fresh SRP acid wastes, respectively.

Oxidation Behavior

Preliminary tests on the oxidation behavior of cermets have been performed. Upon an 8-hour exposure at 770 K in air, a uniform oxide film

approximately 2 μm in thickness formed on the surfaces. A 2-hour exposure to air at 1070 K resulted in an oxide layer approximately 5-7 μm thick. As expected, the oxidation behavior of cermets is primarily dependent upon the metal matrix composition, which in these cases was 70 wt. % Fe, 20 wt. % Ni, 5 wt. % Cu, and 5 wt. % Co.

Thermal Shock Resistance

Throughout laboratory handling of samples, cermets have shown no susceptibility to damage caused by thermal shock. In a brief quantitative test series, cermet samples were cycled three times between 1200 K and a water quench. Since the 1200 K heating was performed in air, an oxide film formed on the surface; however, metallographic examination of the samples revealed no damage or alteration of the cermets as a result of this severe thermal shock.

APPLICATION OF CERMETS TO SPACE DISPOSAL OF NUCLEAR WASTES

Battelle Columbus Laboratories (BCL), under contract to NASA Marshall Space Flight Center has been conducting a technical evaluation of space disposal of radioactive wastes [11]. Until recently, these studies were constrained to waste forms for which industrial scale processing would be developed by the early 1980's. This essentially precluded consideration of any alternative waste forms except calcine and glass. These latter waste forms are considered to be unsatisfactory for this purpose since they fail to meet requirements specific to the space disposal concept. New studies have been initiated that are targeted to include those commercial and/or defense high-level waste forms whose

related technologies are expected to be available in the mid 1990's. This decision permits consideration of a wide variety of waste forms, many of which are only in early stages of development. Recently, at a peer review meeting of representatives from a variety of sites* the cermet solid waste form was selected, by consensus, as the most practical candidate for the space disposal option. Outlined below are desirable waste form features and their weighting by relative importance by which the alternative forms were evaluated.

1. High waste loading - higher waste loadings reduce the number of launches required for a given amount of waste with resultant cost reduction. Rating: primary importance.
2. High thermal conductivity - good heat transfer ability is required both to prevent excessively high centerline temperatures resulting from high heat-generating characteristics of commercial waste and to rapidly conduct heat away from the waste form surface in the event of unplanned reentry of an unprotected waste package. Rating: primary importance.
3. Resistance to thermal shock - resistance to fracture under thermal shock is the key to achieving low dispersibility of waste under abortive conditions. Rating: secondary importance.
4. Thermochemical stability - considering dispersion under abortive conditions, the waste form must possess thermochemical stability. Rating: primary importance.

*Included were representatives from ONWI, DOE, NASA, BCL, INEL, ORNL, PNL, and Sandia.

5. Resistance to leaching - while leach resistance is important, it is not as critical as in the case of terrestrial disposal. In the event of an accident, the unprotected waste form package could impact in water, thus requiring some resistance to leaching. In many reentry scenarios, however, the waste form will remain protected by a reentry package and flotation collar. Rating: secondary importance.
6. Toughness - the waste form should absorb impact without shattering so as to facilitate retrieval and resist dispersion of the waste. Rating: primary importance.
7. Applicability to both commercial and defense HLW mixes - for the purpose of this study, the waste form should be applicable to "clean" wastes from commercial and defense sources. Rating: primary importance.
8. Fabrication technology - the ability to form large shapes (spheres or cylinders, 1-meter diameter) by remote processing in a reliable fashion by the the mid 1990's. Rating: primary importance.
9. Economics - waste form materials and processing should not be prohibitively expensive; however, in relation to the cost of a single launch, this will not be a controlling factor. Rating: secondary importance.
10. Resistance to oxidation - in the event of unplanned reentry of an unshielded waste package, the waste form surface should not rapidly oxidize nor break away from the main body of the waste package causing dispersion.

While waste forms containing metal are susceptible to oxidation, their high thermal conductivity minimizes surface temperature by conducting heat away and thus reduces oxidation and fragmenting of the main body of the waste package. Rating: secondary importance.

Waste forms evaluated under this set of criteria were the ORNL cermet, ICPP glass ceramic, Sandia titanate ceramic, borosilicate glass, metal matrix (coated particle) and pressed supercalcine. Because of density and waste loading requirements, concrete and Synroc waste forms were not included in this review. Of the waste forms listed, the ORNL cermet possessed the optimum rating for the overall list of requirements for space disposal [12]. A detailed engineering evaluation of the application of the cermet waste form to the disposal of HLW in space is currently in progress by NASA and its subcontractor, Battelle Columbus Laboratories.

ACKNOWLEDGMENTS

The authors would like to acknowledge the assistance provided by J. A. Setaro and ORNL's Operations Division and Metals and Ceramics Division in the work performed on actual high-level wastes during this program. Significant contributions to the development of the cermet waste form were made by D. K. Thomas, D. W. Ramey and M. Petek of IRML and Clarence Guyer of ORNL's Operations Division. Professor Donald Kinser of Vanderbilt University provided a great deal of assistance to this program as an Oak Ridge Associated Universities (ORAU) research participant. Finally, the authors gratefully acknowledge the work of B. A. Caylor throughout the program for the preparation of reports, papers and all miscellaneous data presentations associated with this program.

REFERENCES

1. W. S. Aaron, T. C. Quinby, E. H. Kobisk, Cermet High-Level Waste Forms, ORNL/TM-6404, June 1978.
2. T. C. Quinby, "Neutron Dosimetry", U. S. Patent 3,971,944, 1976.
3. T. C. Quinby, "Method of Producing Mixed Metal Oxides and Metal-Metal Oxide Mixtures", U. S. Patent 4,072,501, 1978.
4. M. M. Abraham, L. A. Boatner, T. C. Quinby, D. K. Thomas, M. Rappaz, "Preparation and Compaction of Synthetic Monazite Powders", American Ceramic Society's 1980 Annual Meeting, April 27-30, 1980, Chicago, Illinois.
5. R. Lim, R. Elson, C. L. Hoenig, R. Otto, C. Slettevold, "Powder Preparation for Ceramic Waste Form Synthesis by Means of Urea Coprecipitation", American Ceramic Society's 1980 Annual Meeting, April 27-30, 1980, Chicago, Illinois.
6. M. S. Hanson, C. A. Knox, D. N. Berger, Design Features of the Laboratory-Scale Radiochemical Immobilization System, PNL-3027, Pacific Northwest Laboratory, May 1980.
7. W. S. Aaron, T. C. Quinby, E. H. Kobisk, "Development and Characterization of Cermet Forms for Radioactive Waste", Scientific Basis for Nuclear Waste Management, edited by C. J. Northrup (Plenum Press, New York, 1980), Vol. 2.
8. W. D. Jones, Fundamental Principles of Powder Metallurgy, Edward Arnold Publishers Ltd., London (1960).
9. J. H. Westsik, R. P. Turcotte, Hydrothermal Reactions of Nuclear Waste Solids, A Preliminary Study, PNL-2759, Pacific Northwest Laboratory, September 1978.

10. The Evaluation and Review of Alternative Waste Forms for Immobilization of High-Level Radioactive Wastes, Alternative Waste Form Peer Review Panel, L. L. Hench, Chairman, U. S. Department of Energy Report DOE/TIC-10228 (1979).
11. K. R. Yates, "Waste Mixes and Forms for Space Disposal of Nuclear Waste", Transactions American Nuclear Society, 33 (1979) 436-437.
12. Analysis of Nuclear Waste Disposal in Space-Phase III, Vols. 1 and 2, Battelle Columbus Laboratories, NASA CR 161418 and 161419, (1980).

INTERNAL DISTRIBUTION

- | | | | |
|--------|-------------------|--------|--------------------------------|
| 1. | W. S. Aaron | 35. | K. J. Notz |
| 2. | H. L. Adair | 36. | M. Petek |
| 3. | P. Angelini | 37. | H. Postma |
| 4. | E. C. Beahm | 38. | T. C. Quinby |
| 5. | R. E. Blanco | 39. | D. W. Ramey |
| 6. | J. O. Blomeke | 40. | T. H. Row |
| 7. | L. A. Boatner | 41. | C. D. Scott |
| 8. | W. D. Burch | 42. | J. A. Setaro |
| 9. | D. E. Ferguson | 43. | D. P. Stinton |
| 10. | W. J. Frederick | 44. | S. M. Tiegs |
| 11. | H. W. Godbee | 45. | D. B. Trauger |
| 12. | R. K. Kibbe | 46. | M. K. Wilkinson |
| 13-27. | E. H. Kobisk | 47. | R. G. Wymer |
| 28. | F. A. Kocur | 48. | F. W. Young, Jr. |
| 29. | W. J. Lackey | 49. | A. Zucker |
| 30. | T. B. Lindemer | 50-52. | Central Research Library |
| 31. | A. P. Malinauskas | 53. | Document Reference Section |
| 32. | E. W. McDaniel | 54-73. | Laboratory Records Department |
| 33. | J. G. Moore | 74. | Laboratory Records Dept., R.C. |
| 34. | E. Newman | 75. | ORNL Patent Office |

EXTERNAL DISTRIBUTION

- 76-77. S. W. Ahrends, Director, Nuclear Research and Development Division, Oak Ridge Operations Office, U. S. Department of Energy, Oak Ridge, Tennessee 37830
78. S. R. Ali-Zaidi, Glass Containers Corporation, 114 Pen Avenue, Knox, Pennsylvania 16232
79. A. D. Baranyi, Ontario Research Foundation, Mississauga, Ontario, Canada L5K 1B3
80. C. B. Bartlett, Chief, Fuel Cycle Research Branch, Division of Fuel Cycle and Environmental Research, U. S. Nuclear Regulatory Commission, Mail Stop SS 1130, Washington, D.C. 20555
81. S. J. Beard, Fuel Reprocessing Engineering, Exxon Nuclear Company, Inc., 777 106th Avenue, N.E., Bellevue, Washington 98009
82. M. M. Beary, Rockwell Hanford Operations, Richland, Washington 99352
83. W. F. Bennett, Acting Director, Fuels and Components Division, Office of Light Water Reactors, Rocky Flats Area Office P. O. Box 928, Golden, Colorado 80401
84. Ralph Best, ONWI, Battelle Columbus Laboratories, 505 King Avenue, Columbus, Ohio 43201

85. P. T. Bickman, EG&G Idaho, Inc., P. O. Box 1625, Idaho Falls, Idaho 83401
86. W. F. Bonner, Manager, Nuclear Waste Process Development, P. O. Box 999, Pacific Northwest Laboratories, Richland, Washington 99352
87. J. W. Braithwaite, Sandia Laboratories, Albuquerque, New Mexico 87185
88. R. A. Brown, Exxon Nuclear Idaho Company, Inc., P. O. Box 2800, Idaho Falls, Idaho 83401
89. J. A. Buckman, Allied-General Nuclear Services, P. O. Box 847, Barnwell, South Carolina 29812
90. J. L. Burnett, Division of Physical Research, U. S. Department of Energy, Germantown, Maryland 20767
91. J. Campbell, Project Leader, University of California, Lawrence Livermore Laboratory, P. O. Box 808, L-224, Livermore, California 94550
92. R. H. Campbell, U. S. Department of Energy, Albuquerque Operations Office, P. O. Box 5400, Albuquerque, New Mexico 87115
93. W. A. Carbiener, Office of Nuclear Waste Isolation, Battelle Columbus Laboratories, 505 King Avenue, Columbus, Ohio 43201
94. R. Carricaburn, Hennisson Durham Richardson, 804 Anacopa St., Santa Barbara, California 93101
95. P. R. Compton, Code RES-1, NASA Headquarters, Washington, D.C. 20540
96. F. R. Cook, Nuclear Regulatory Commission, HLW Licensing Branch, Materials Section, Washington, D.C. 20555
97. C. R. Cooley, Acting Director, Research and Development Division, Office of Waste Isolation, Mail Stop B-107, NE 331, U. S. Department of Energy, Washington, D. C. 20545
98. W. R. Cornman, Savannah River Plant, Aiken, South Carolina 29801
99. J. L. Crandall, Director, Savannah River Laboratory, P. O. Box A, Aiken, South Carolina 29801
100. S. J. Creamer, Purdue University, 2595 Yeager Road, West Lafayette, Indiana 47906

- 101-102. G. H. Daly, Acting Director, Waste Technology Branch, Division of Waste Products, Office of Nuclear Waste Management, Mail Stop B-107 (ET-952), U. S. Department of Energy, Washington, D.C. 20545
103. R. Danford, Attn: Input Processing Division, Institute Research and Evaluation, 21098 Control Center, Eagen, Minnesota 55121
104. M. M. Dare, Oak Ridge Operations Office, U. S. Department of Energy, Oak Ridge, Tennessee 37830
105. P. T. Dickman, EG&G Idaho, Inc., P. O. Box 1625, Idaho Falls, Idaho 83401
106. J. E. Dieckhoner, Director, Operations Division, Office of Waste Operations and Technology, Nuclear Waste Programs, U. S. Department of Energy, NE-321, Mail Stop B-107, Germantown, Maryland 20545
- 107-108. Director, Nuclear Research and Development Division, U. S. Department of Energy, Oak Ridge Operations, Oak Ridge, Tennessee 37830
109. W. Drent, Eurchemic Library, B-2400 Mol, Belgium
110. J. P. Duckworth, Nuclear Fuel Services, Inc., P. O. Box 124, West Valley, New York 14171
- 111-112. O. J. Elgert, Richland Operations Office, U. S. Department of Energy, Richland, Washington 99352
113. K. Flynn, Argonne National Laboratory, 9700 South Cass Ave., Argonne, Illinois 60439
- 114-116. R. G. Garvin, Savannah River Laboratories, P. O. Box A, Aiken, South Carolina 29801
117. E. Goldberg, Chief of Waste Management, Savannah River Operations Office, P. O. Box A, Aiken, South Carolina 29801
118. D. E. Gordon, Savannah River Laboratories, P. O. Box A, Aiken, South Carolina 29801
119. Harry Groh, E. I. du Pont de Nemours & Co., Inc., Savannah River Plant, Aiken, South Carolina 29801
120. W. Haller, U. S. Department of Commerce, National Bureau of Standards, Washington, D.C. 20234
121. J. P. Hamric, Director, Nuclear Fuel Cycle and Waste Management Division, Idaho Operations Office, Department of Energy, 550 Second Street, Idaho Falls, Idaho 83401

- 122-123. S. G. Harbinson, San Francisco Operations, U. S. Department of Energy, 1333 Broadway, Oakland, California 94612
124. E. C. Hardin, Albuquerque Operations Office, U. S. Department of Energy, P. O. Box 5400, Albuquerque, New Mexico 87115
125. W. S. Harmon, Fossil Energy, Major Facility Project Management, U. S. Department of Energy, Washington, D.C. 20545
126. Art Hathaway, Boeing Engineering and Construction, Mail Stop 9A48, ORG. K4510, P. O. Box 3707, Seattle, Washington 98124
127. P. J. Hayward, AECL, Whiteshell Nuclear Research Establishment, Pinawa, Manitoba, Canada ROE 1L0
128. C. A. Heath, Director, Office of Waste Isolation, NE-330, Mail Stop B-107, U. S. Department of Energy, Germantown, Maryland 20545
129. L. L. Hench, Department of Materials Science & Engineering, University of Florida, Gainesville, Florida 32611
130. L. R. Hill, Supervisor, Nuclear Waste Technology Division, Sandia Laboratories, Albuquerque, New Mexico 87115
131. T. B. Hindman, Jr., Deputy Director, Waste Management Program Office, Savannah River Operations Office, U. S. Department of Energy, P. O. Box A, Aiken, South Carolina 29801
132. C. Hoenig, University of California, Lawrence Livermore Laboratory, Livermore, California 94550
133. International Atomic Energy Agency, Kartner Ring 11, P. O. Box 509, A-1011 Vienna, Austria
134. L. J. Jardine, Argonne National Laboratory, 9700 South Cass Ave., Argonne, Illinois 60439
135. B. F. Judson, General Electric Company, 175 Curtner Avenue, M/C 858, San Jose, California 95125
136. E. L. Keller, Oak Ridge Operations Office, U. S. Department of Energy, P. O. Box E, Oak Ridge, Tennessee 37830
137. R. G. Kepler, Organic and Electronic, Department 5810, Sandia Laboratories, Albuquerque, New Mexico 87185
- 138-139. J. H. Kittel, Office of Waste Management Programs, Argonne National Laboratory, 9700 South Cass Avenue, Argonne, Illinois 60439
140. J. C. Landers, Acting Director Financial Management Division, Office of Resource Management and Planning, Mail Stop B-107, U. S. Department of Energy, Germantown, Maryland 20545

141. J. L. Landon, Program Manager for Surplus-Facilities Management, Richland Operations Office, U. S. Department of Energy, P. O. Box 550, Richland, Washington 99352
142. L. Lani, Chief, Waste Management Nuclear Magnetic Fusion Division, NE-31, San Francisco Operations Office, U. S. Department of Energy, 1333 Broadway, Oakland, California 94612
- 143-144. D. E. Large, Program Manager, Radioactive Waste Program, U. S. Department of Energy, Oak Ridge Operations, Oak Ridge, Tennessee 37830
145. M. J. Lawrence, Acting Director, Office of the Director, Office of Transportation and Fuel Storage, NE-34, Mail Stop B-107, U. S. Department of Energy, Germantown, Maryland 20545
146. W. H. Lewis, Vice President, Nuclear Fuel Services, Inc., 6000 Executive Blvd., Rockville, Maryland 20852
- 147-148. R. Y. Lowrey, Chief, Waste Management Branch, Weapons Production Division, Albuquerque Operations Office, U. S. Department of Energy, P. O. Box 5400, Albuquerque, New Mexico 87115
149. R. Maher, Program Manager, Waste Management Programs, E. I. du Pont de Nemours & Co., Savannah River Plant, Aiken, South Carolina 29801
150. S. A. Mann, Technical Manager, Sodium Waste Technology, Chicago Operations and Regional Office, U. S. Department of Energy, 900 South Cass Avenue, Argonne, Illinois 60439
- 151-152. A. B. Martin, Rockwell International, Energy Systems Group, 8900 DeSoto Avenue, Conoga Park, California 91304
153. J. Martin, Director for Waste Management, Division of Fuel Cycle and Material Safety, U. S. Nuclear Regulatory Commission, Washington, D.C. 20555
154. E. F. Mastel, Planning and Analysis Division, Office of Resource Management and Planning, Mail Stop B-107, U. S. Department of Energy, Germantown, Maryland 20545
155. M. D. McCormack, EG&G Idaho, Inc., P. O. Box 1625, Idaho Falls, Idaho 83401
156. W. R. McDonell, SRL, Aiken, South Carolina 29801
157. J. L. McElroy, Pacific Northwest Laboratories, Battelle Boulevard, Richland, Washington 99352

158. D. J. McGoff, Acting Director, Projects Division, Office of Waste Operations and Technology, U. S. Department of Energy, Mail Stop G-234 (ET-82), Germantown, Maryland 20545
159. D. L. McIntosh, E. I. du Pont de Nemours & Co., Savannah River Laboratory, Aiken, South Carolina 29801
160. J. E. Mendel, Pacific Northwest Laboratories, Battelle Boulevard, Richland, Washington 99352
161. S. Meyers/R. Romatowski, Office of Nuclear Waste Management, U. S. Department of Energy, Mail Stop B-107 (ET-90), Germantown, Maryland 20545
162. A. D. Miller, EPRI, 3412 Hillview Ave., P. O. Box 10412, Palo Alto, California 94303
163. M. A. Molecke, Nuclear Waste Technology Division, Sandia Laboratories, Albuquerque, New Mexico 87115
164. J. O. Neff, Program Manager, NWTs Program Office, U. S. Department of Energy, 505 King Avenue, Columbus, Ohio 43201
165. N. Naito, Mitsui and Co., Inc., 200 Park Avenue, New York, New York 10017
- 166-168. R. D. Nelson, Manager, Nuclear Waste Materials Characterization Center, Battelle Project Office, 505 King Avenue, Columbus, Ohio 43201
- 169-173. G. K. Oertel, Director, Office of Waste Products, Mail Stop B-107, U. S. Department of Energy, Washington, D.C. 20545
174. Office of Assistant Manager, Energy Research and Development, U. S. Department of Energy, Oak Ridge Operations, Oak Ridge, Tennessee 37830
175. D. A. Orth, Savannah River Plant, E. I. du Pont de Nemours & Co., Inc., Aiken, South Carolina 29801
176. Hayne Palmour III, North Carolina State University, 2140 Burlington Engineering Laboratories, Raleigh, N. C. 27607
177. Professor L. F. Pau, Ambassade de France Aux Etats-Unis., Services de la Mission Scientifique, 2 129 Wyoming Avenue, N.W., Washington, D.C. 20008
178. H. Pearlman, Rockwell Energy Systems Group, P. O. Box 309, Canoga Park, California 91305

179. J. W. Peel, Program Manager, National Low-Level Waste Programs Branch, Nuclear Fuel Cycle Division, Idaho Operations Office, U. S. Department of Energy, 550 Second Street, Idaho Falls, Idaho 83401
180. T. C. Petit, Laboratoire Rene-Bernas, Batiment 108 Boite Postale 1, 91406 Orsay, France
- 181-183. A. M. Platt, Battelle-Pacific Northwest Laboratory, P. O. Box 999, Richland, Washington 99352
184. R. G. Post, College of Engineering, University of Arizona, Tucson, Arizona 85721
185. C. C. Priest, NASA, Marshall Space Flight Center, Huntsville, Alabama 35812
186. R. W. Ramsey, Acting Program Manager, Remedial Action Program, Division of Waste Products, NE-30, Mail Stop B-107, U. S. Department of Energy, Germantown, Maryland 20545
187. G. L. Rogosa, Division of Physical Research, U. S. Department of Energy, Washington, D.C., 29545
188. D. M. Rohrer, U.S. Nuclear Regulatory Commission, Washington, D.C. 20545
189. D. M. Roy, Materials Research Laboratory, Pennsylvania State University, University Park, Pennsylvania 16802
190. R. Roy, Materials Research Laboratory, Pennsylvania State University, University Park, Pennsylvania 16802
191. Professor Guna Salvaduray, Materials Engineering, San Jose State University, San Jose, California 95192
192. J. T. Schriber, Manager, Waste Management Division, Richland Operations Office, U. S. Department of Energy, Richland, Washington 99352
193. L. W. Scully, Nuclear Waste Technology Division, Sandia Laboratories, Sandia, New Mexico 87115
194. J. J. Shefcik, General Atomic Company, P. O. Box 81608, San Diego, California 92138
195. C. Sombret, Centre de Marcoule, B.P. 170, 30200 Bagnols-Sur-Ceze, France

196. M. J. Steindler, Argonne National Laboratory, Chemical Engineering Division, 9700 South Cass Avenue, Argonne, Illinois 60439
197. D. K. Stevens, Director, Division of Material Sciences, Office of Basic Energy Sciences, Office of Energy Research, U. S. Department of Energy, Washington, D.C. 20545
198. A. C. Sugarman, Science Applications, Inc., Palo Alto, California 94304
199. A. L. Taboas, TRU Program Manager, Waste Management Branch, U. S. Department of Energy, Albuquerque Operations Office, P. O. Box 5400, Albuquerque, New Mexico 87115
200. J. D. Thompson, EG&G Idaho, Inc., P. O. Box 1625, Idaho Falls, Idaho 83401
201. R. E. Tomlinson, Manager, Exxon Nuclear Company, Inc., 2101 Horn Rapids Road, Richland, Washington 99352
202. R. D. Walton, Jr., Technology Branch, Office of Waste Operation and Technology, Mail Stop B-107, U. S. Department of Energy, Washington, D.C. 20545
- 203-204. J. B. Whitsett, Chief, Radioactive Waste Programs Branch, Nuclear Fuel Cycle Division, Idaho Operations Office, U. S. Department of Energy, 550 2nd Street, Idaho Falls, Idaho 83401
205. A. G. Wikjord, AECL, Whiteshell Nuclear Research Establishment, Pinawa, Manitoba, Canada ROE 1L0
- 206-208. D. D. Wodrich, Rockwell Hanford Operations, P. O. Box 800, Richland, Washington 99352
209. Ken Yates, Battelle Columbus Laboratories, 505 King Avenue, Columbus, Ohio 43201
- 210-528. Given distribution as shown in TID-4500 under the Nuclear Waste Management Category.